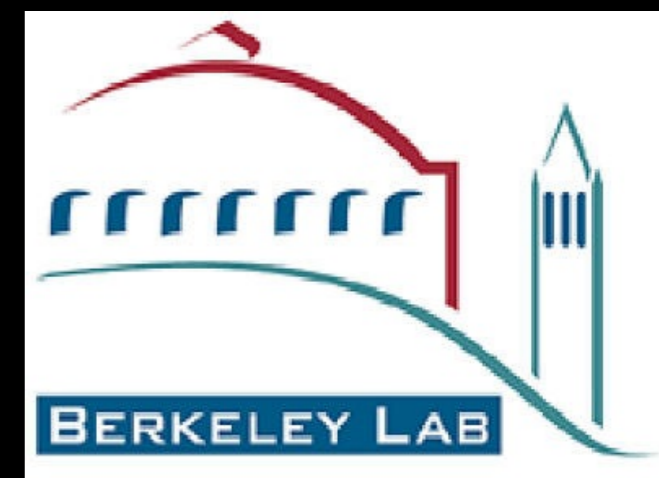




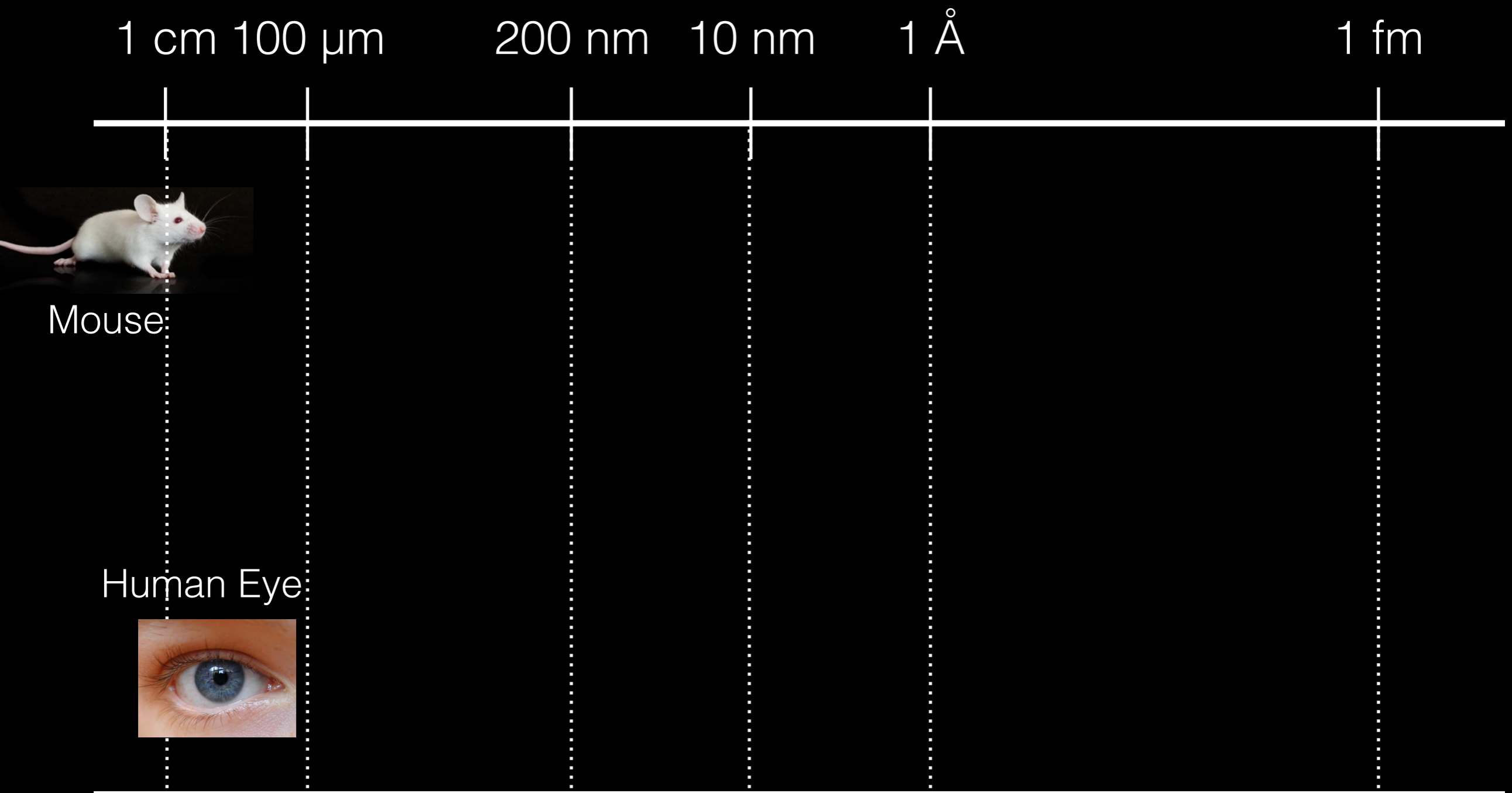
ALICE

Quantum statistics measurements using 2-, 3-, and 4-pion Bose-Einstein correlations

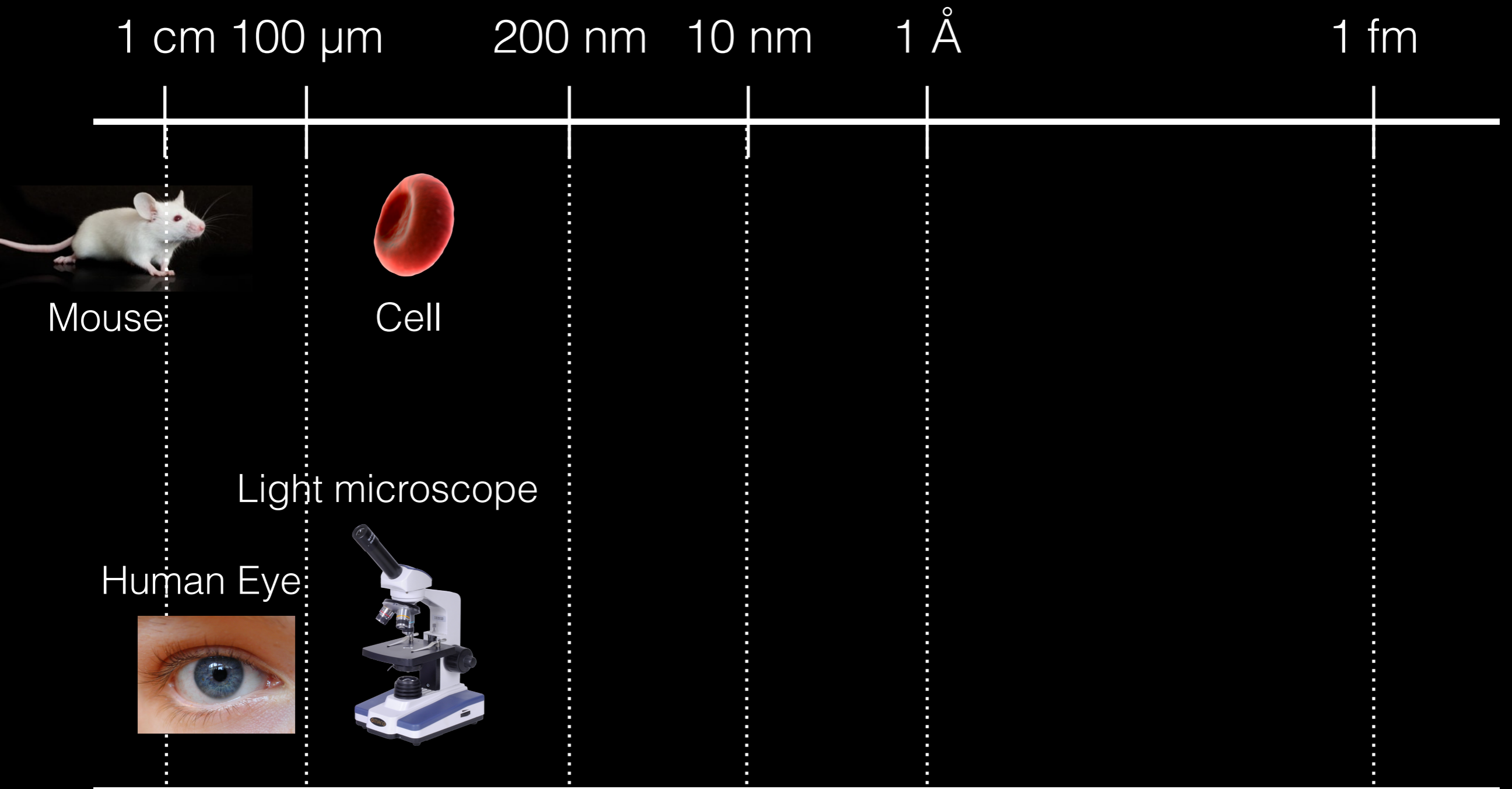
Dhevan Gangadharan (LBNL)
on behalf of the ALICE collaboration
CERN PH seminar, Oct. 14th 2014



Measuring Spatial Structures

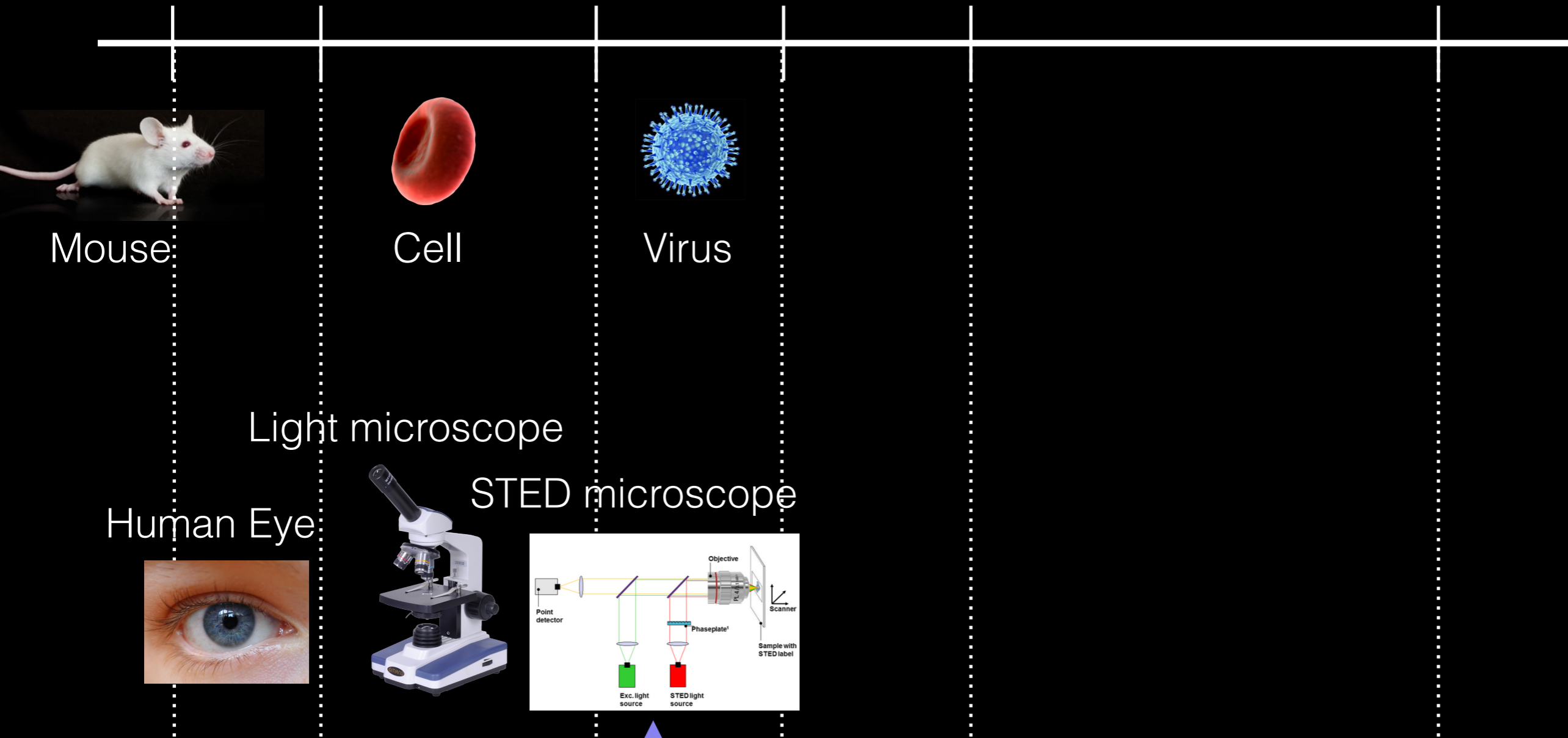


Measuring Spatial Structures



Measuring Spatial Structures

1 cm 100 μm 200 nm 10 nm 1 \AA 1 fm



Mouse

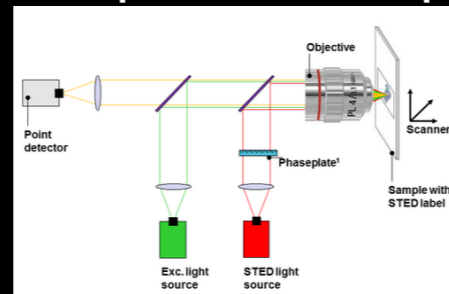
Cell

Virus

Light microscope

STED microscope

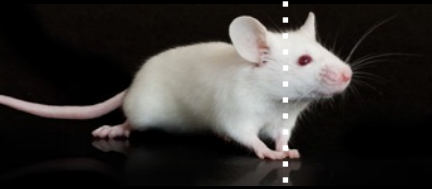
Human Eye



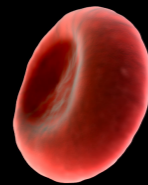
2014 Nobel Prize in Chemistry!

Measuring Spatial Structures

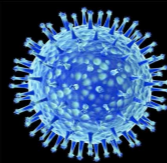
1 cm 100 μm 200 nm 10 nm 1 \AA 1 fm



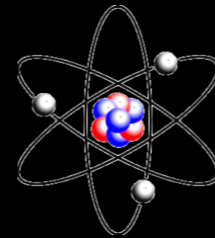
Mouse



Cell



Virus



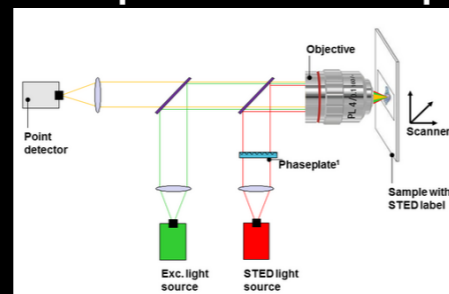
Atom

Light microscope

Electron microscope

Human Eye

STED microscope



2014 Nobel Prize in Chemistry!

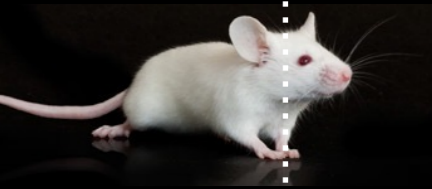
Measuring Spatial Structures

1 cm 100 μm

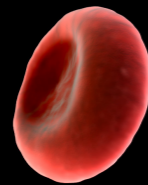
200 nm 10 nm

1 \AA

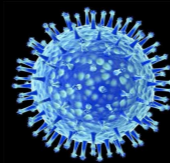
1 fm



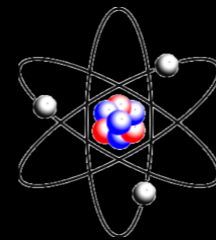
Mouse



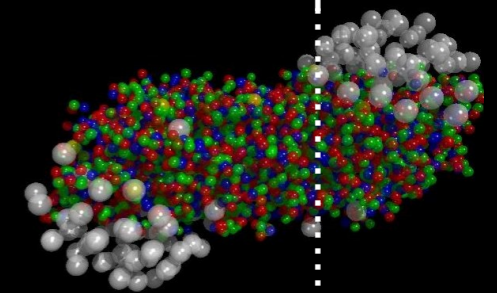
Cell



Virus



Atom



Heavy-ion collisions

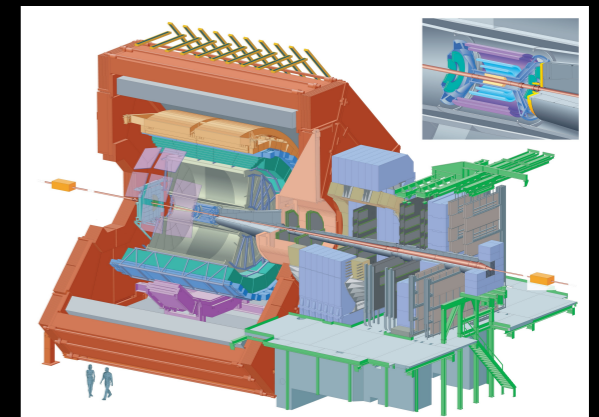
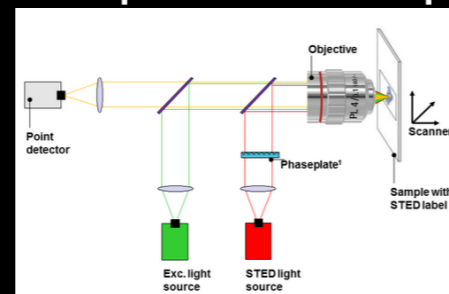
Light microscope

Electron microscope

Tracking detector

Human Eye

STED microscope



2014 Nobel Prize in Chemistry!

Exploiting Quantum Statistics (QS) to measure the source size

- The last stage of particle interactions is freeze-out
- At freeze-out in high-energy particle collisions, the characteristic separation of particles is femtoscopic ($\Delta x \sim 10^{-15}$ m).

$$\Delta x \Delta p \gg 2\pi\hbar$$

Classical:
no observable quantum phenomena

$$\Delta x \Delta p \sim 2\pi\hbar$$

Non Classical:
Bose-Einstein / Fermi-Dirac correlations

- Bose-Einstein correlations will be visible for $\Delta p < \sim 0.5$ GeV/c. Relative momentum correlations are sensitive to the relative separation at freeze out.

Exploiting Quantum Statistics (QS) to measure the source size

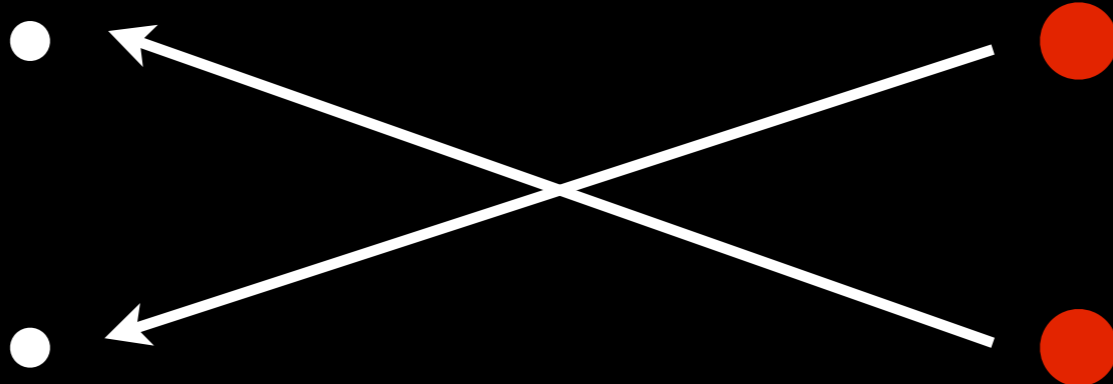
Detection Point

Production Point



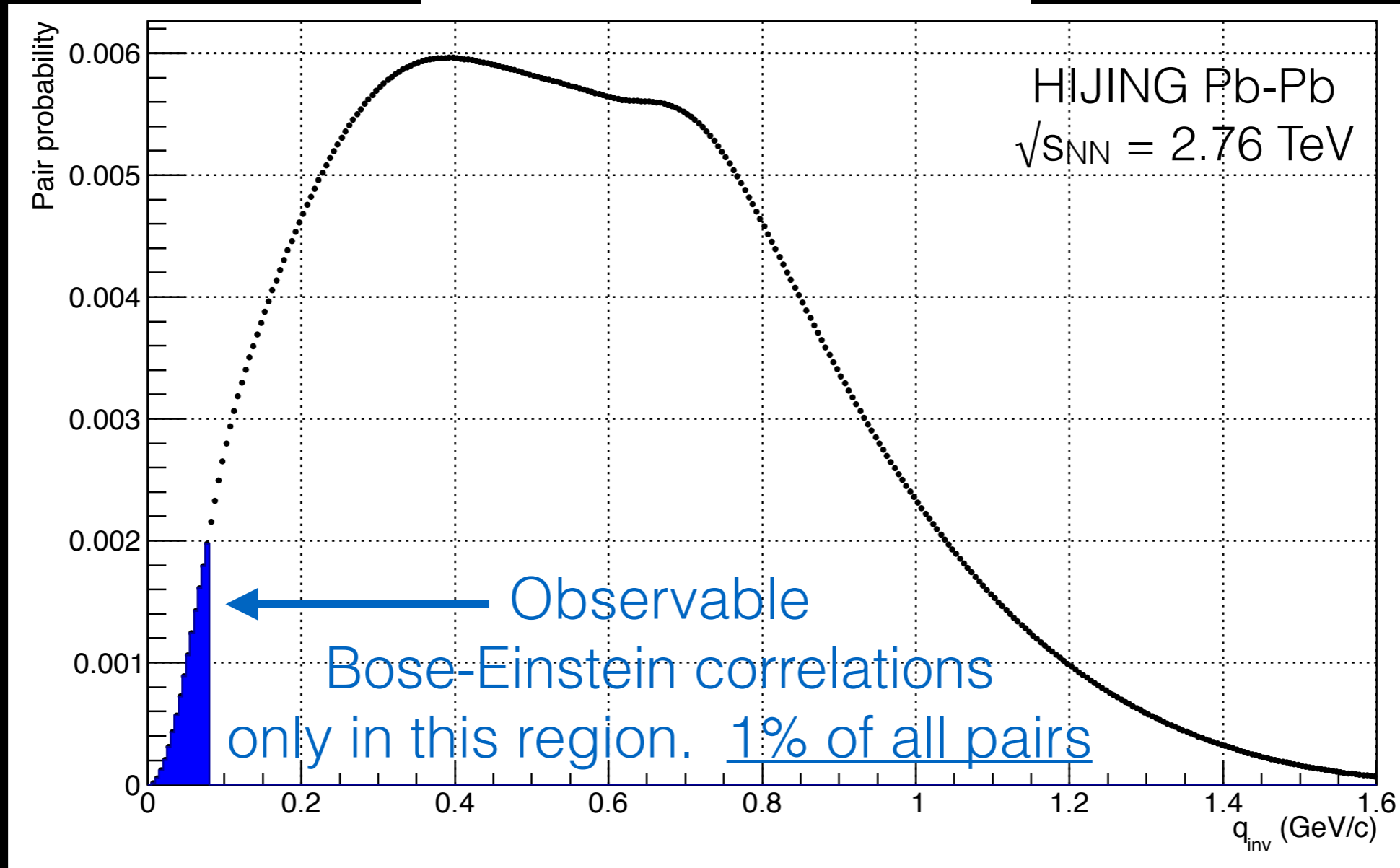
For Indistinguishable
Bosons

+



Bose-Einstein correlations are in a very narrow region of phase-space

$$\Delta x \Delta p \leq 2\pi \hbar$$

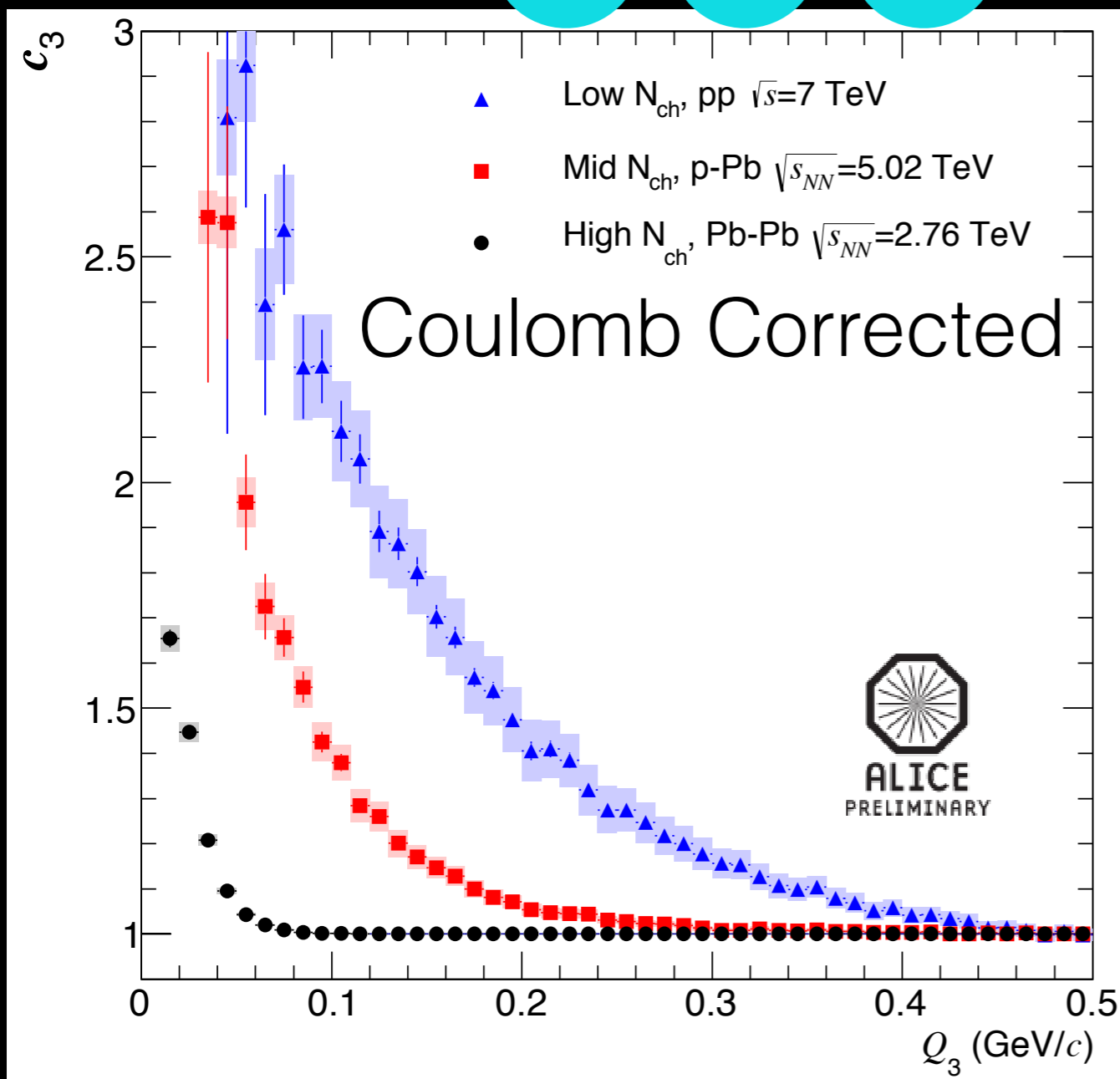


$$q_{inv} = \sqrt{(\vec{p}_1 - \vec{p}_2)^2 - (E_1 - E_2)^2}$$

Femtoscopy (10^{-15})

The study of particle correlations at low relative momentum

3-pion Correlation: π^+ π^+ π^+



Low Q region is dominated by Quantum Statistics (QS) and Coulomb correlations.

Clean region of study

AKA:

Bose-Einstein Correlations
Quantum Statistics Correlations
“HBT” Correlations

= Triplet relative momentum

2 Uses of Femtoscopy

The last stage of particle interactions is “freeze-out”

**Use
1**

Measure:

Space-time structure at freeze-out
(e.g. Radius)

Sensitive to dynamics
of the collision.

(e.g. Hydrodynamics or not?)

**Use
2**

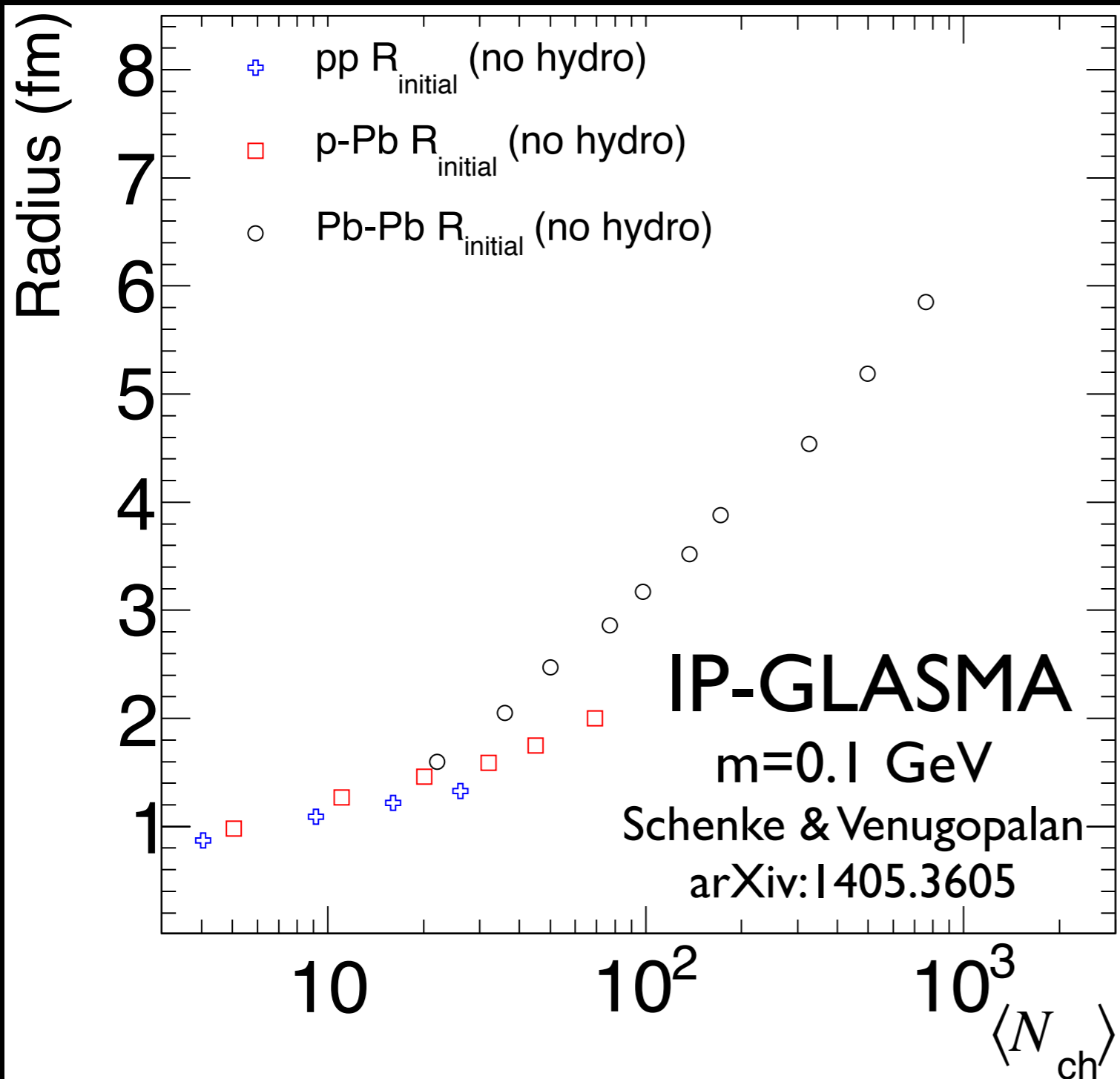
Measure:

Quantum coherence
of particles at freeze-out.

Very sensitive to dynamics of the
collision.

Use 1

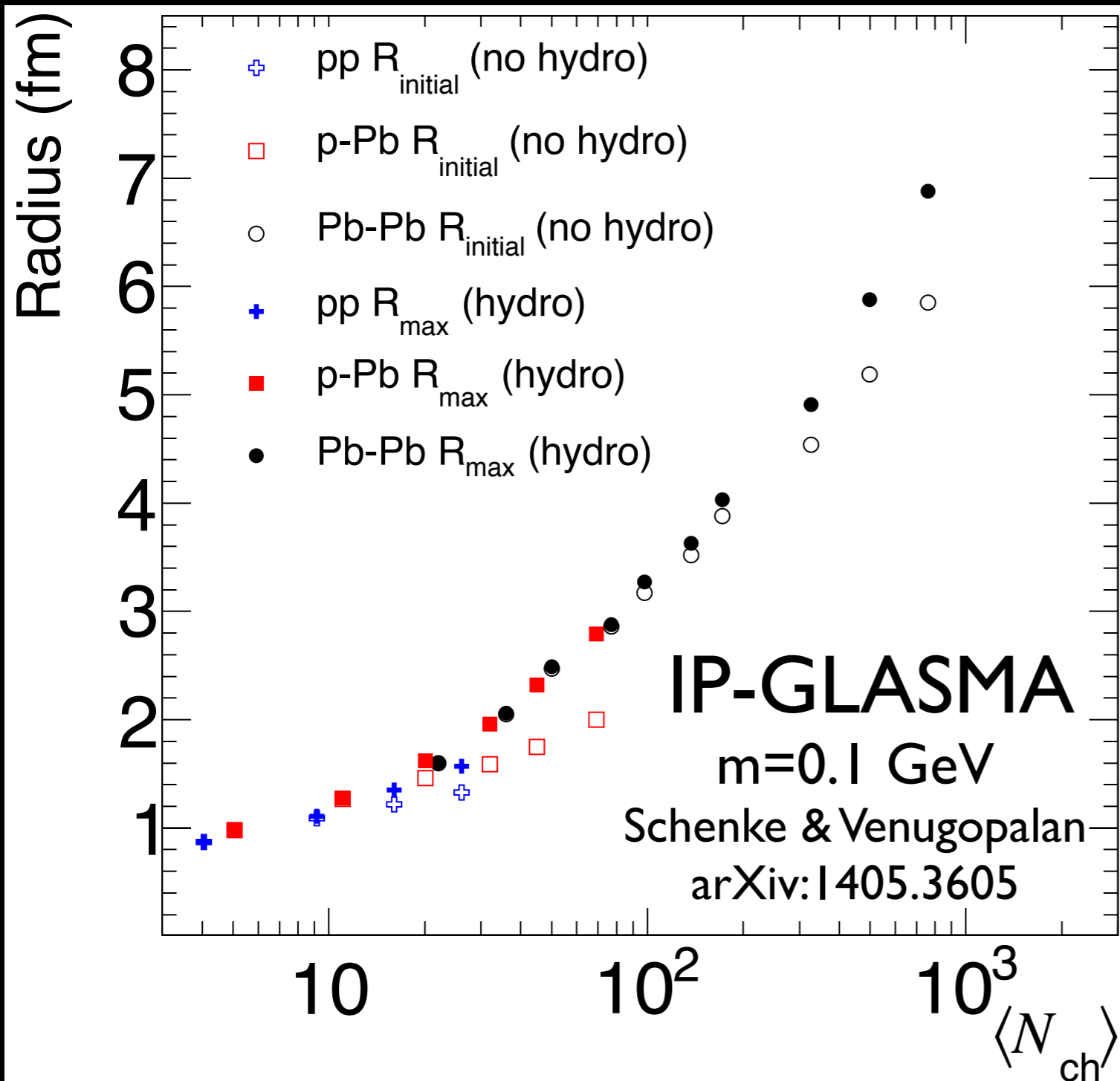
Why is the Source Radius Important



IP-GLASMA initial conditions alone (a model with only gluon fields).
→ Similar freeze-out radius in p-Pb as compared to pp.

Use 1

Why is the Source Radius Important



IP-GLASMA initial conditions alone (a model with only gluon fields).

→ Similar freeze-out radius in p-Pb as compared to pp.

Hydrodynamic expansion

→ Larger freeze-out radius. p-Pb more comparable to Pb-Pb

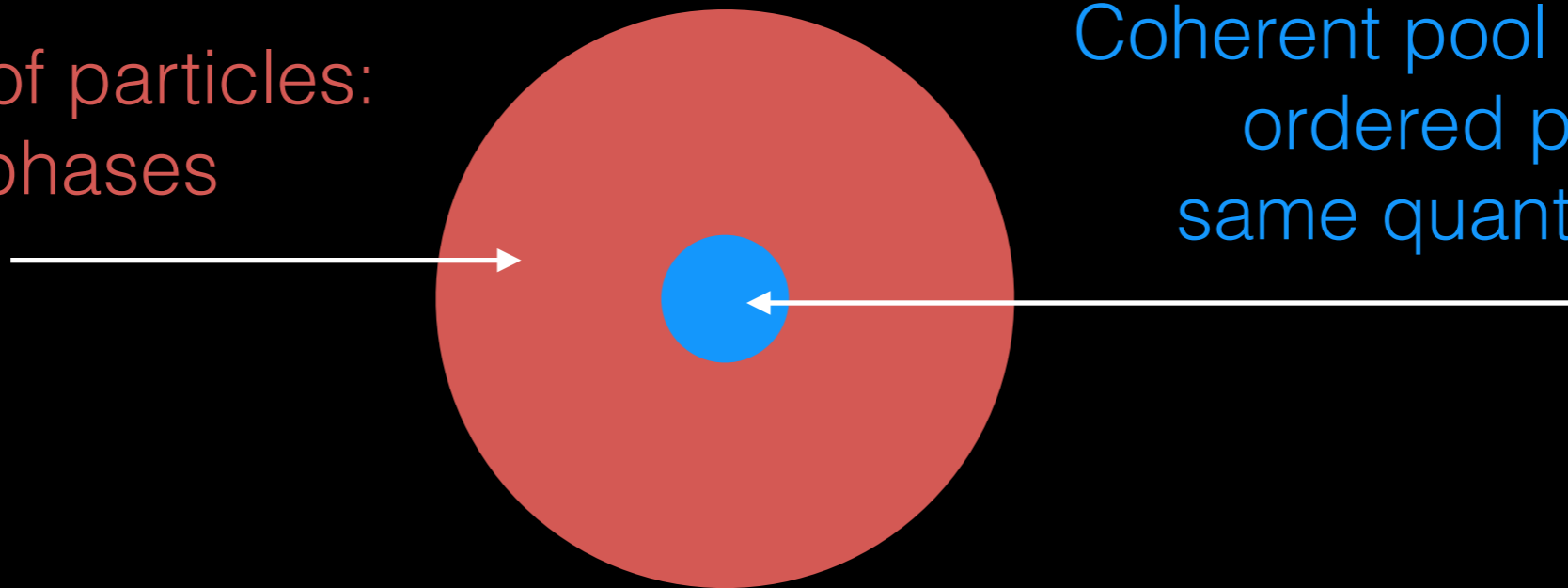
There are other hydrodynamic predictions as well:

Bozek and Broniowski,
Phys. Lett. B 720, 250 (2013)

Use
2

Measuring the Coherent Fraction of Pions

Chaotic pool of particles:
random phases



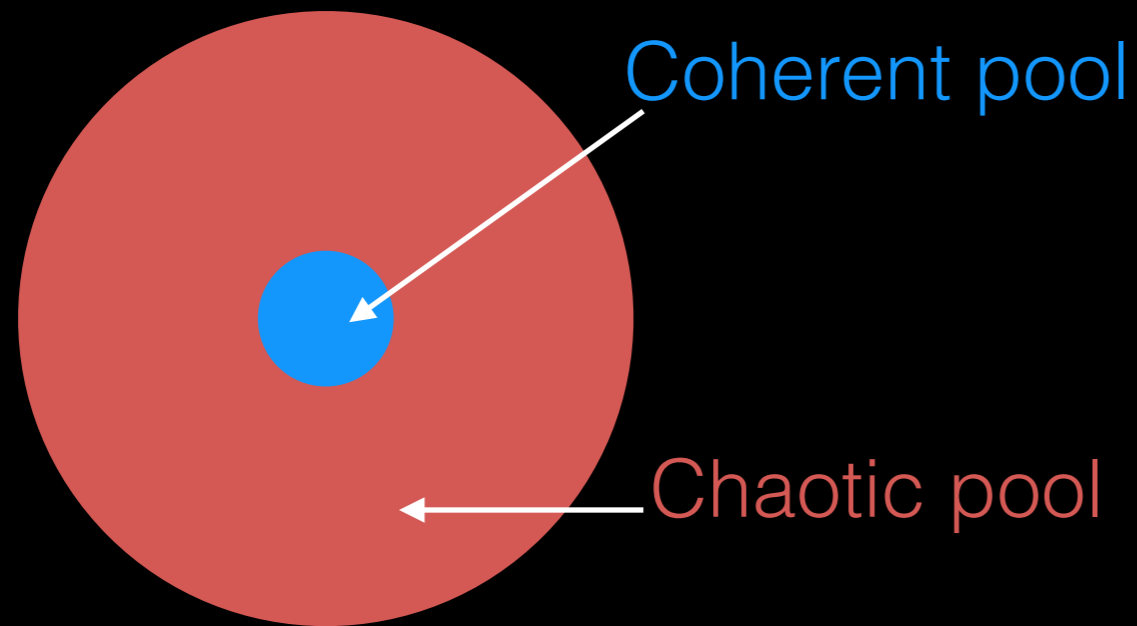
Coherent pool of particles:
ordered phases,
same quantum state

Pion condensation, Disoriented Chiral Condensates, +.....
may create a coherent pool of pions.

For coherence to survive in the final state,
the chaotic pool must not interact with the coherent pool.
Existence of such coherence would imply 2 disjunct sources!

Use
2

2-pion Bose-Einstein Contributions



2-pions

$\pi \pi$

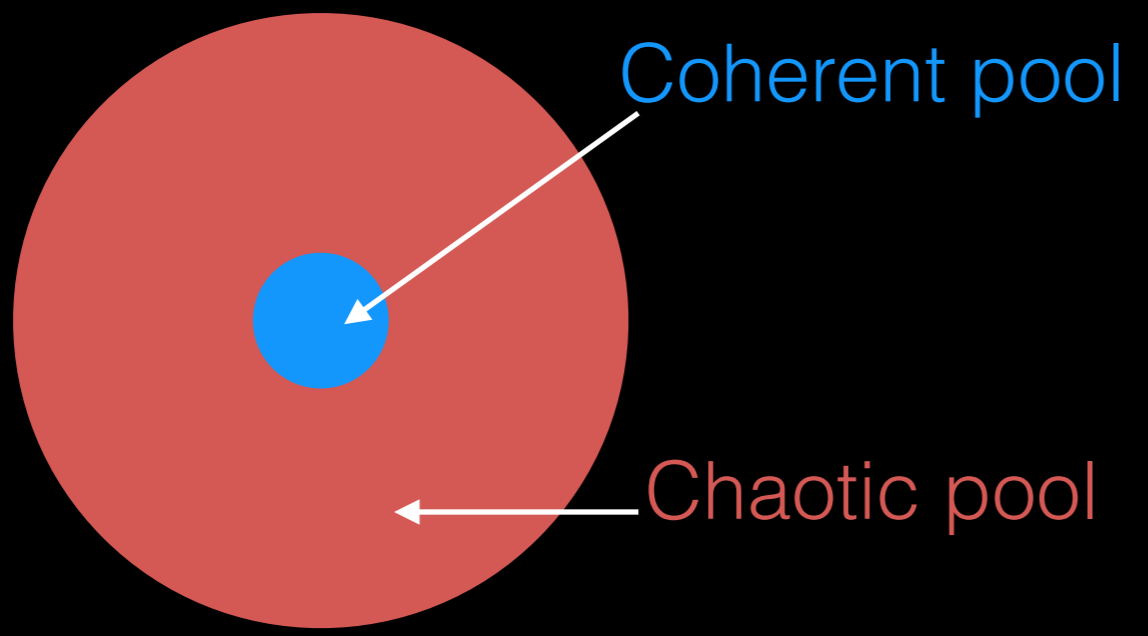
$\pi \pi$

~~$\pi \pi$~~

1 suppressed combination

Use
2

3-pion Bose-Einstein Contributions



3-pions

$\pi \pi \pi$

$\pi \pi \pi$

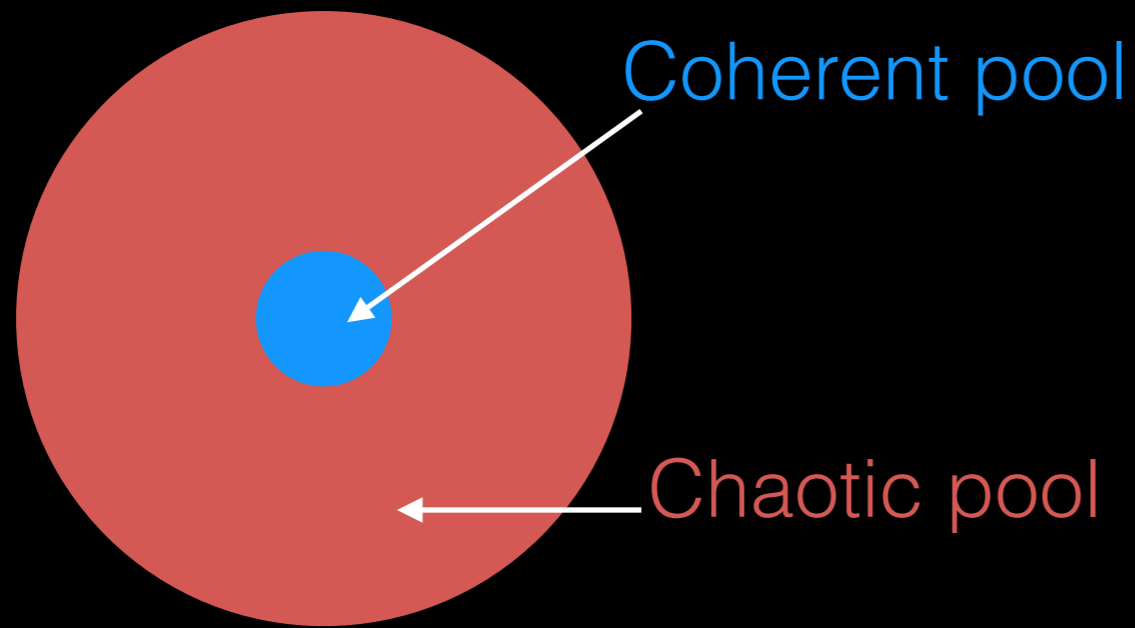
~~$\pi \pi \pi$~~

~~$\pi \pi \pi$~~

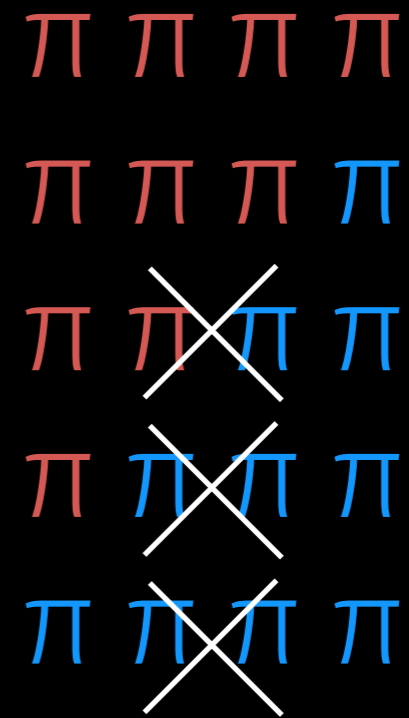
2 suppressed combinations

Use
2

4-pion Bose-Einstein Contributions



4-pions

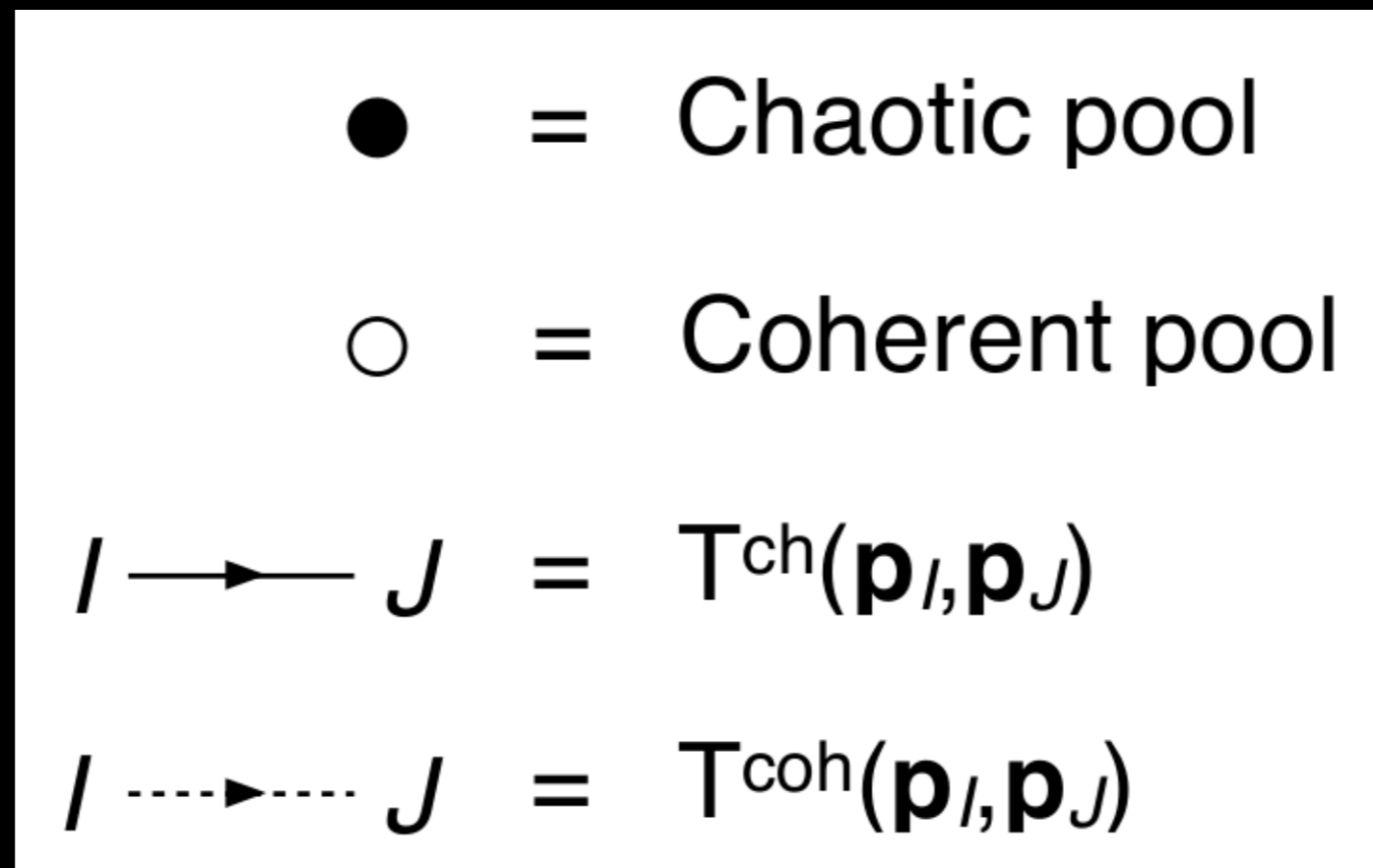


3 suppressed combinations

Resolution of coherence increases with the number of pions used.

Pair Exchange Amplitude

— Building Blocks of Bose-Einstein Correlations



T_{IJ} is the pair exchange amplitude:

Fourier Transform of source space-time distribution.
It is the building-block of all orders of Bose-Einstein correlations.

2-boson Symmetrization

$$C_2 = 1 + \text{Diagram 1} + \text{Diagram 2} + \text{Diagram 3}$$

Diagrams derived from
T. Csorgo
Heavy Ion Physics **15** 1-80

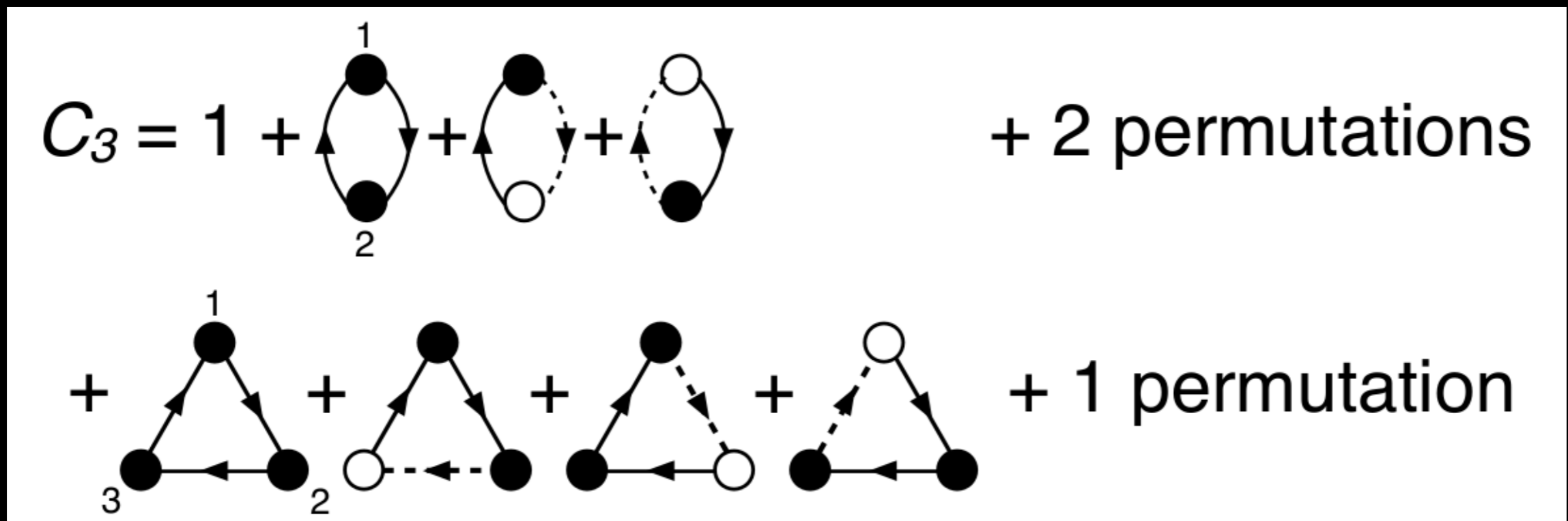
$$C_2(1, 2) = 1 + (1 - G)^2 (T_{12}^{\text{ch}})^2 + 2G(1 - G) T_{12}^{\text{ch}} T_{12}^{\text{coh}} \cos(\phi_{12}^{\text{ch-coh}})$$

coherent fraction of pions

phase of chaotic-coherent
interference.

Equations derived from
I. Andreev et al.
Int. J. Mod. Phys. A **8** 4577

3-boson Symmetrization



Diagrams derived from
 T. Csorgo
 Heavy Ion Physics **15** 1-80

4-boson Symmetrization

$$C_4 = 1 + \begin{array}{c} 1 \\ \bullet \\ \curvearrowright \\ \bullet \\ 2 \end{array} + \begin{array}{c} \bullet \\ \curvearrowright \\ \bullet \\ \curvearrowright \\ \bullet \end{array} + \begin{array}{c} \bullet \\ \curvearrowright \\ \circ \\ \curvearrowright \\ \bullet \end{array}$$

+ 5 permutations

$$+ \begin{array}{c} 1 \\ \bullet \\ \curvearrowright \\ \bullet \\ 2 \end{array} \begin{array}{c} 3 \\ \bullet \\ \curvearrowright \\ \bullet \\ 4 \end{array} + \begin{array}{c} \bullet \\ \curvearrowright \\ \bullet \\ \curvearrowright \\ \bullet \end{array} \begin{array}{c} \bullet \\ \curvearrowright \\ \bullet \\ \curvearrowright \\ \bullet \end{array} + \begin{array}{c} \bullet \\ \curvearrowright \\ \circ \\ \curvearrowright \\ \bullet \end{array} \begin{array}{c} \bullet \\ \curvearrowright \\ \bullet \\ \curvearrowright \\ \bullet \end{array} + \begin{array}{c} \bullet \\ \curvearrowright \\ \bullet \\ \curvearrowright \\ \bullet \end{array} \begin{array}{c} \bullet \\ \curvearrowright \\ \circ \\ \curvearrowright \\ \bullet \end{array} + \begin{array}{c} \bullet \\ \curvearrowright \\ \bullet \\ \curvearrowright \\ \bullet \end{array} \begin{array}{c} \bullet \\ \curvearrowright \\ \circ \\ \curvearrowright \\ \bullet \end{array} + \begin{array}{c} \bullet \\ \curvearrowright \\ \circ \\ \curvearrowright \\ \bullet \end{array} \begin{array}{c} \bullet \\ \curvearrowright \\ \bullet \\ \curvearrowright \\ \bullet \end{array}$$

+ 2 permutations

$$+ \begin{array}{c} 1 \\ \bullet \\ \nearrow \\ \bullet \\ 3 \end{array} \begin{array}{c} \bullet \\ \searrow \\ \bullet \\ 2 \end{array} + \begin{array}{c} \bullet \\ \nearrow \\ \bullet \\ \searrow \\ \bullet \end{array} \begin{array}{c} \bullet \\ \searrow \\ \bullet \\ 2 \end{array} + \begin{array}{c} \bullet \\ \nearrow \\ \bullet \\ \searrow \\ \bullet \end{array} \begin{array}{c} \bullet \\ \searrow \\ \circ \\ 2 \end{array} + \begin{array}{c} \bullet \\ \nearrow \\ \bullet \\ \searrow \\ \bullet \end{array} \begin{array}{c} \bullet \\ \searrow \\ \bullet \\ 2 \end{array}$$

+ 7 permutations

$$+ \begin{array}{c} 1 \\ \bullet \\ \rightarrow \\ \bullet \\ 4 \end{array} \begin{array}{c} 2 \\ \bullet \\ \rightarrow \\ \bullet \\ 3 \end{array} + \begin{array}{c} \bullet \\ \rightarrow \\ \bullet \\ \rightarrow \\ \bullet \end{array} \begin{array}{c} \bullet \\ \rightarrow \\ \bullet \\ \rightarrow \\ \bullet \end{array} + \begin{array}{c} \bullet \\ \rightarrow \\ \bullet \\ \rightarrow \\ \bullet \end{array} \begin{array}{c} \bullet \\ \rightarrow \\ \circ \\ \rightarrow \\ \bullet \end{array} + \begin{array}{c} \bullet \\ \rightarrow \\ \bullet \\ \rightarrow \\ \bullet \end{array} \begin{array}{c} \bullet \\ \rightarrow \\ \bullet \\ \rightarrow \\ \bullet \end{array} + \begin{array}{c} \bullet \\ \rightarrow \\ \bullet \\ \rightarrow \\ \bullet \end{array} \begin{array}{c} \bullet \\ \rightarrow \\ \bullet \\ \rightarrow \\ \bullet \end{array}$$

+ 5 permutations

*Diagrams derived from
T. Csorgo
Heavy Ion Physics **15** 1-80*

Standard Correlation Functions

$$C_n = \frac{N_n(\mathbf{p}_1, \mathbf{p}_2, \dots, \mathbf{p}_n)}{N_1(\mathbf{p}_1)N_1(\mathbf{p}_2)\dots N_1(\mathbf{p}_n)}$$

\mathbf{p} = momentum

Projection Variables

$$q_{ij} = \sqrt{-(p_i - p_j)_\mu (p_i - p_j)^\mu}$$

$$k_T = |\vec{p}_{T1} + \vec{p}_{T2}|/2$$

$$Q_3 = \sqrt{q_{12}^2 + q_{13}^2 + q_{23}^2}$$

$$K_{T,3} = |\vec{p}_{T1} + \vec{p}_{T2} + \vec{p}_{T3}|/3$$

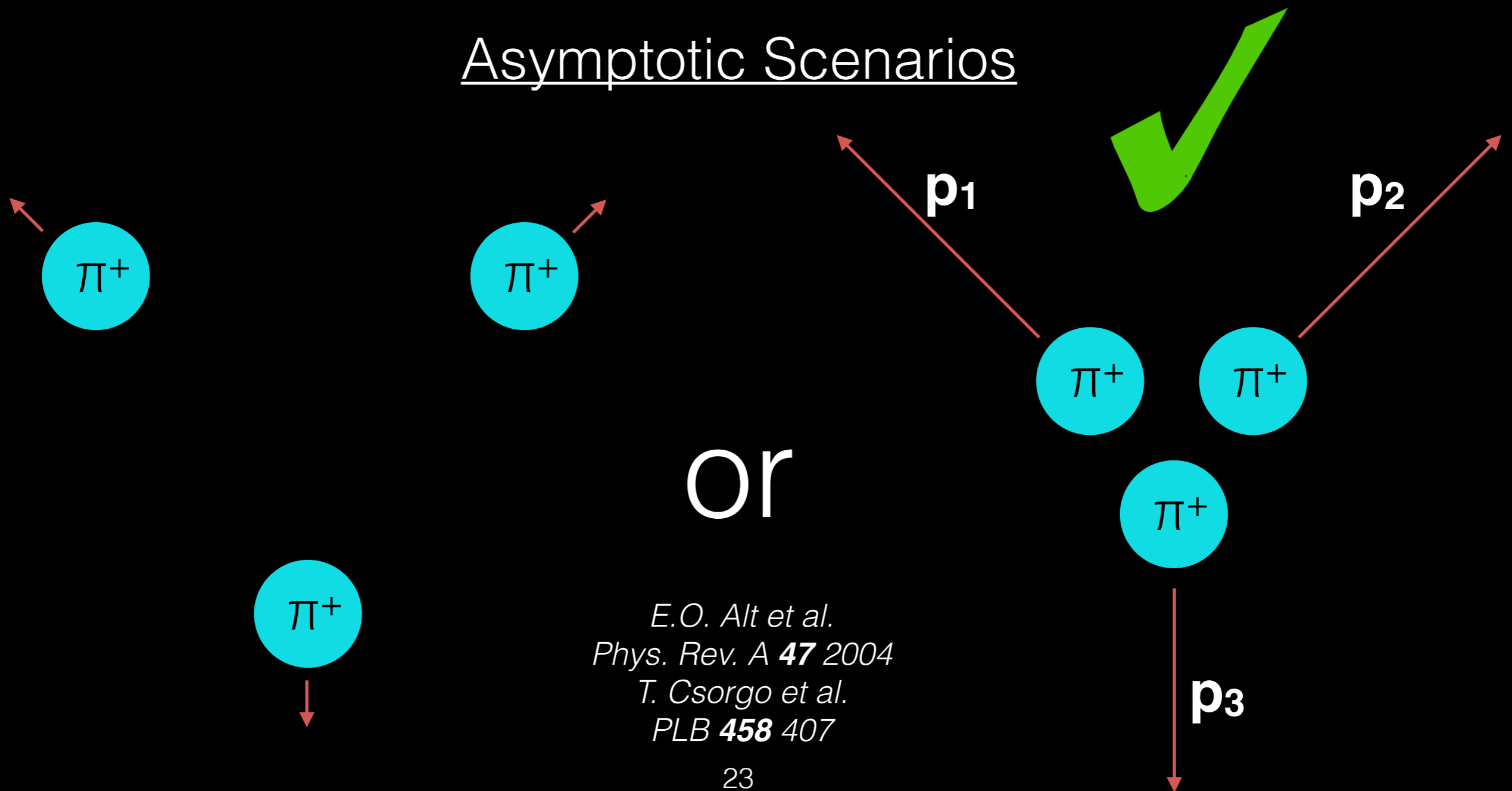
$$Q_4 = \sqrt{q_{12}^2 + q_{13}^2 + q_{14}^2 + q_{23}^2 + q_{24}^2 + q_{34}^2}$$

$$K_{T,4} = |\vec{p}_{T1} + \vec{p}_{T2} + \vec{p}_{T3} + \vec{p}_{T4}|/4$$

Multi-Pion Coulomb Interaction

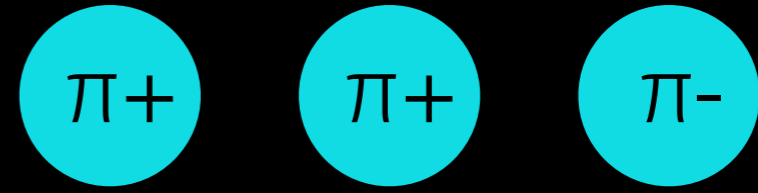
Multi-body Coulomb wave-functions are not known exactly. However, asymptotic solutions exist which are applicable to high-energy collisions.

Asymptotic Scenarios



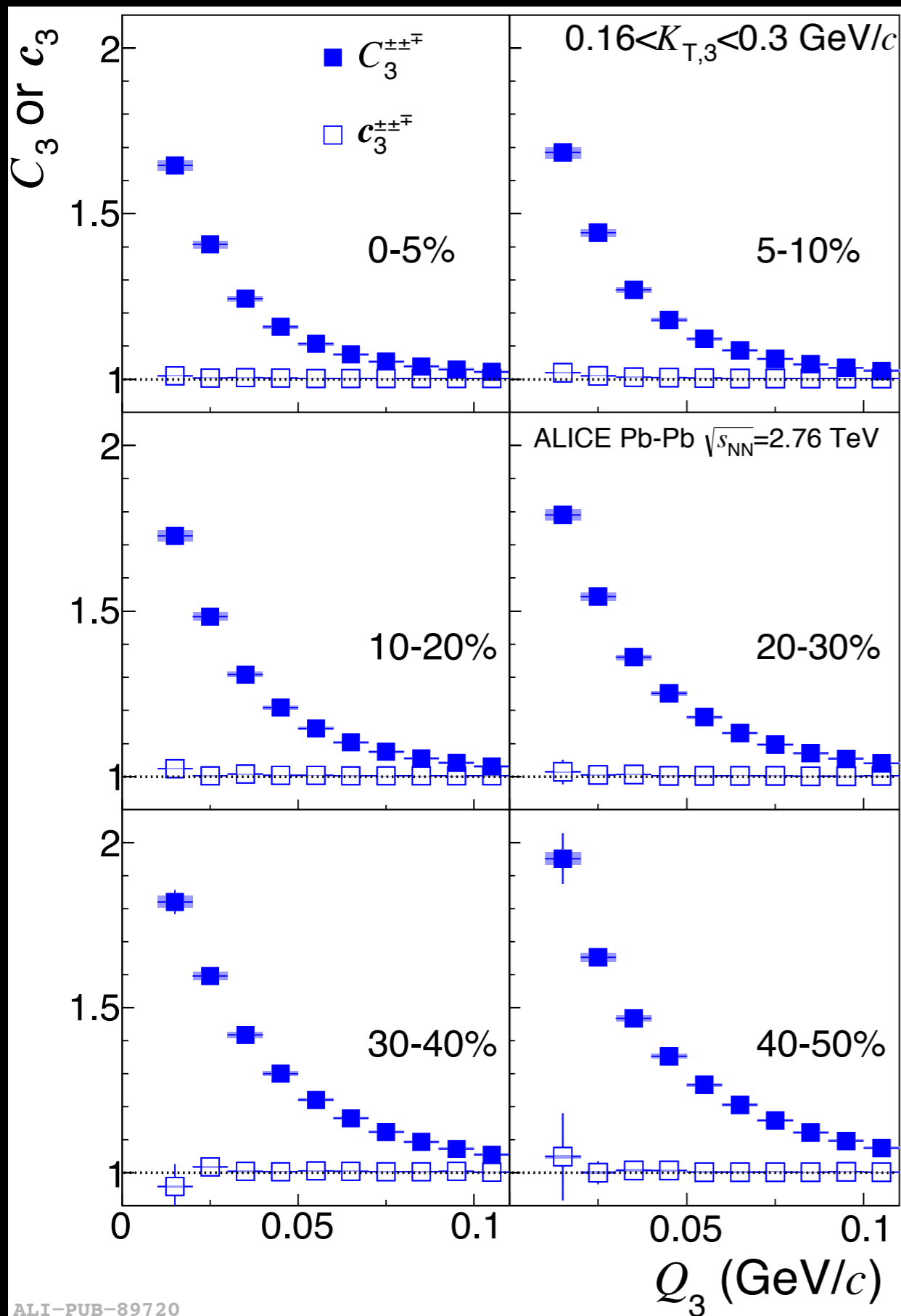
E.O. Alt et al.
Phys. Rev. A **47** 2004
T. Csorgo et al.
PLB **458** 407

Check that 3-body Coulomb corrections work

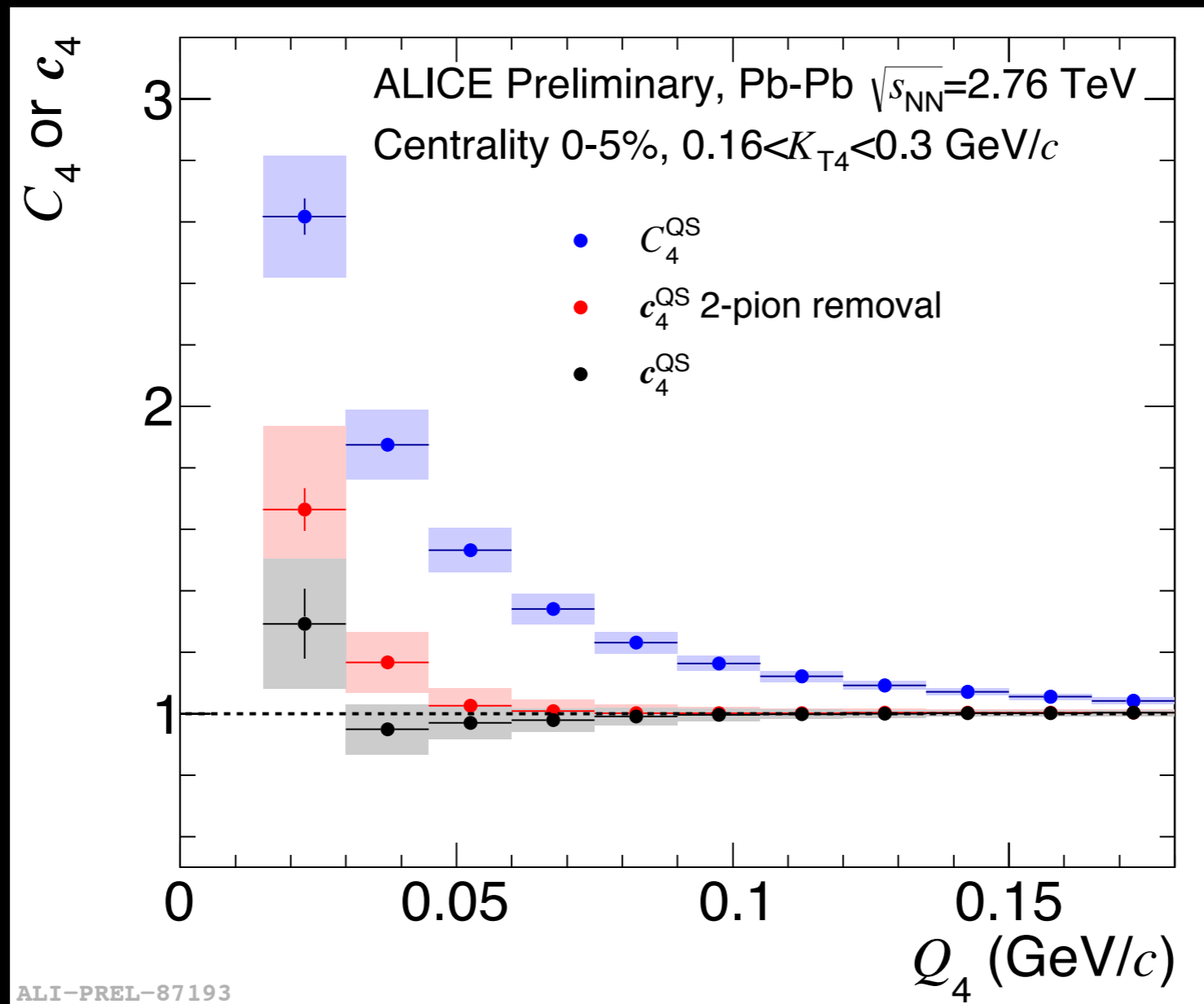
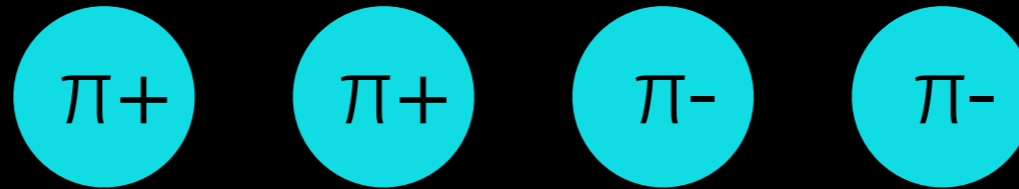


The cumulant (hollow points) are Coulomb corrected.

Consistency with unity demonstrates success of 3-body Coulomb ansatz

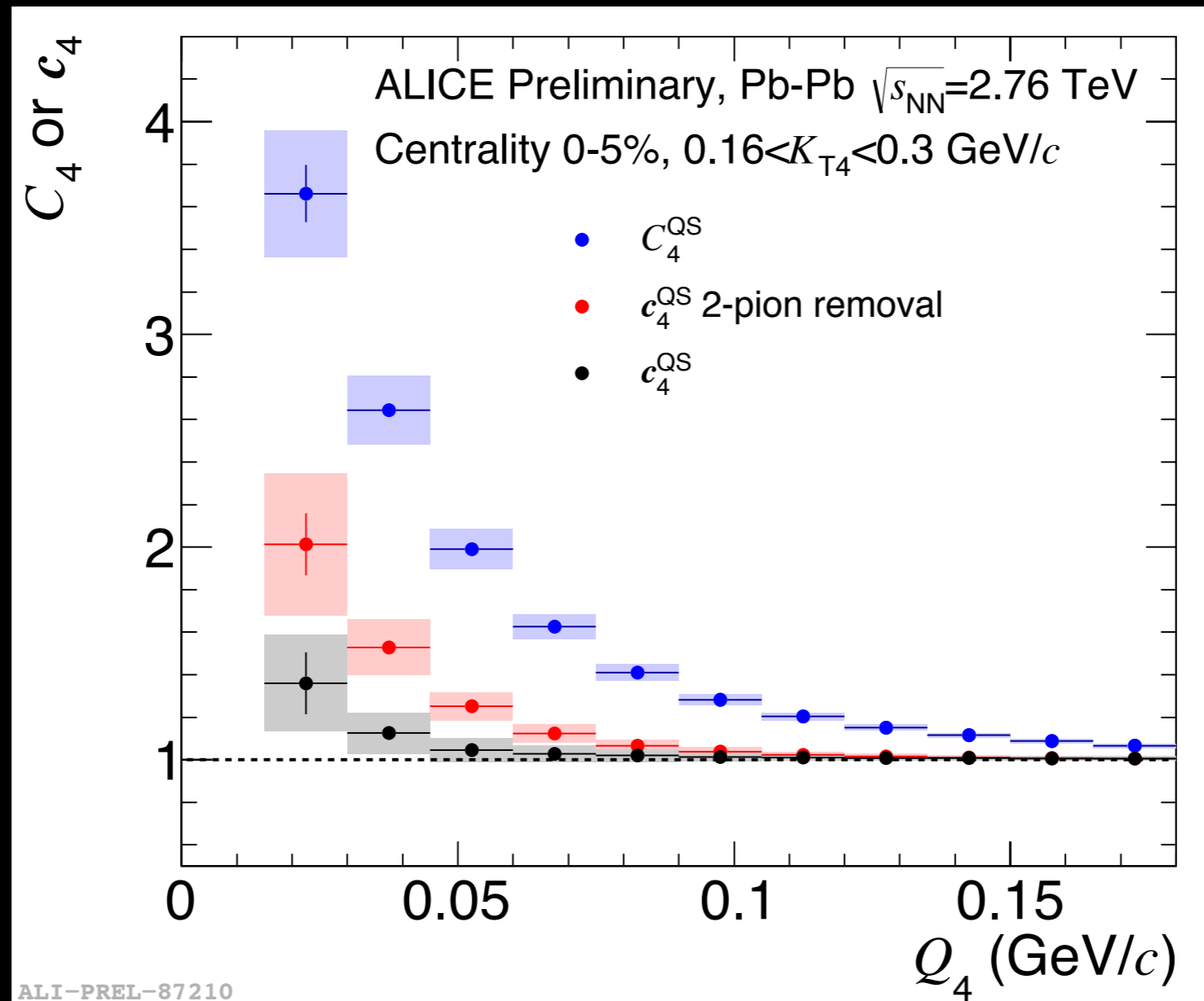
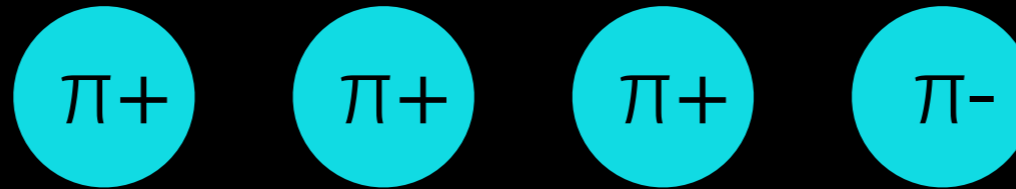


New: 4-pion Coulomb Check



- - - + + correlation well understood. Cumulant (black) near unity.

New: 4-pion Coulomb Check



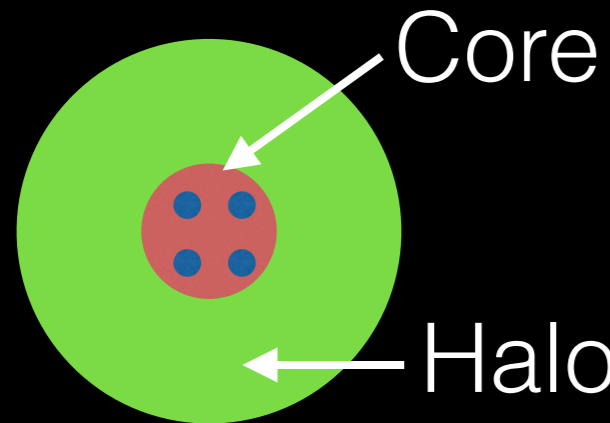
- - - - + correlation mostly understood. Cumulant (black) near unity.
- Ongoing studies in pp and p-Pb suggest that the residue is not Coulomb related.

Dilution from non-Femtoscopic Pairs

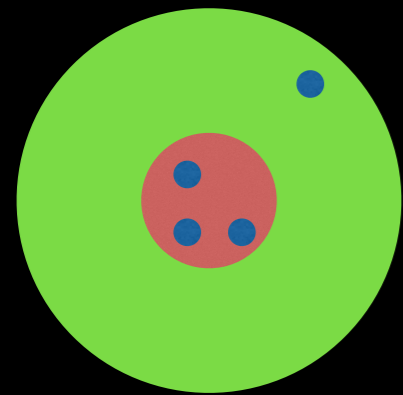
For pairs with relative separation $\gtrsim 50$ fm
there is no observable Bose-Einstein correlation.

4-pion possibilities in the Core/Halo picture

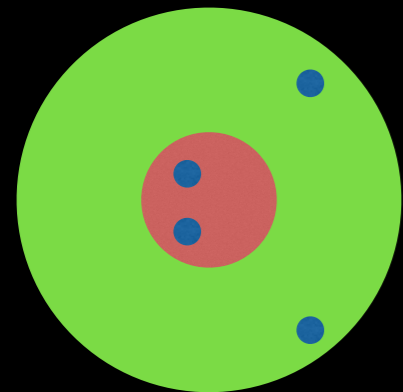
T. Csorgo et al.
Z. Phys. C **71** 491



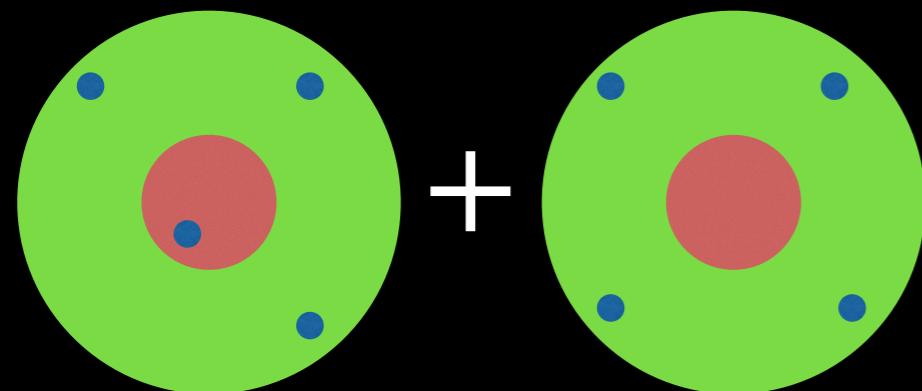
All 4 originating from the core (short-lived emitters)



3 originating from the core



2 originating from the core



1 or 0 originating from the core.
No observable Bose-Einstein correlations

Multi-pion Distributions

4-pion Distributions

- $N_4(p_1, p_2, p_3, p_4)$ — 4 pions from same event
- $N_3(p_1, p_2, p_3) N_1(p_4)$ — 3 pions from same event
- $N_2(p_1, p_2) N_1(p_3) N_1(p_4)$ — 2 pions from same event
- $N_2(p_1, p_2) N_2(p_3, p_4)$ — 2 pairs from same event
- $N_1(p_1) N_1(p_2) N_1(p_3) N_1(p_4)$ — All from different events
- $K_4 = K_2^{12} K_2^{13} K_2^{14} K_2^{23} K_2^{24} K_2^{34}$ — 4-body Final-State-Interaction

Isolation of 4-pion QS

Quantity of Interest



$$\begin{aligned} N_4(p_1, p_2, p_3, p_4) &= f_{41} N_1(p_1) N_1(p_2) N_1(p_3) N_1(p_4) \\ &+ f_{42} N_2(p_1, p_2) N_1(p_3) N_1(p_4) \\ &+ f_{43} N_3(p_1, p_2, p_3) N_1(p_4) \\ &+ f_{44} K_4(q_{12}, q_{13}, q_{14}, q_{23}, q_{24}, q_{34}) N_4^{QS}(p_1, p_2, p_3, p_4) \end{aligned}$$

$$f_{41}^{Core/Halo} = -3(1 - f_c)^4 - 8f_c(1 - f_c)^3 + 6(1 - f_c^2)(1 - f_c)^2$$

$$f_{42}^{Core/Halo} = -6(1 - f_c)^2$$

$$f_{43}^{Core/Halo} = 4(1 - f_c)$$

$$f_{44}^{Core/Halo} = f_c^4.$$

$f_c^2 = \text{"lambda"} = 0.7 \pm 0.05$ (fraction of correlated pairs)

Data and Track Selection

Collision types

$$pp \sqrt{s} = 7 \text{ TeV}$$

$$p\text{-Pb } \sqrt{s_{NN}} = 5.02 \text{ TeV}$$

$$Pb\text{-Pb } \sqrt{s_{NN}} = 2.76 \text{ TeV}$$

Track Selection

- Pions selected based on their specific energy loss in the Time Projection Chamber.

Time of Flight also used for $p > 0.6 \text{ GeV}/c$.

- $p_T > 0.16 \text{ GeV}/c$
- $p < 1.0 \text{ GeV}/c$
- $|\eta| < 0.8$

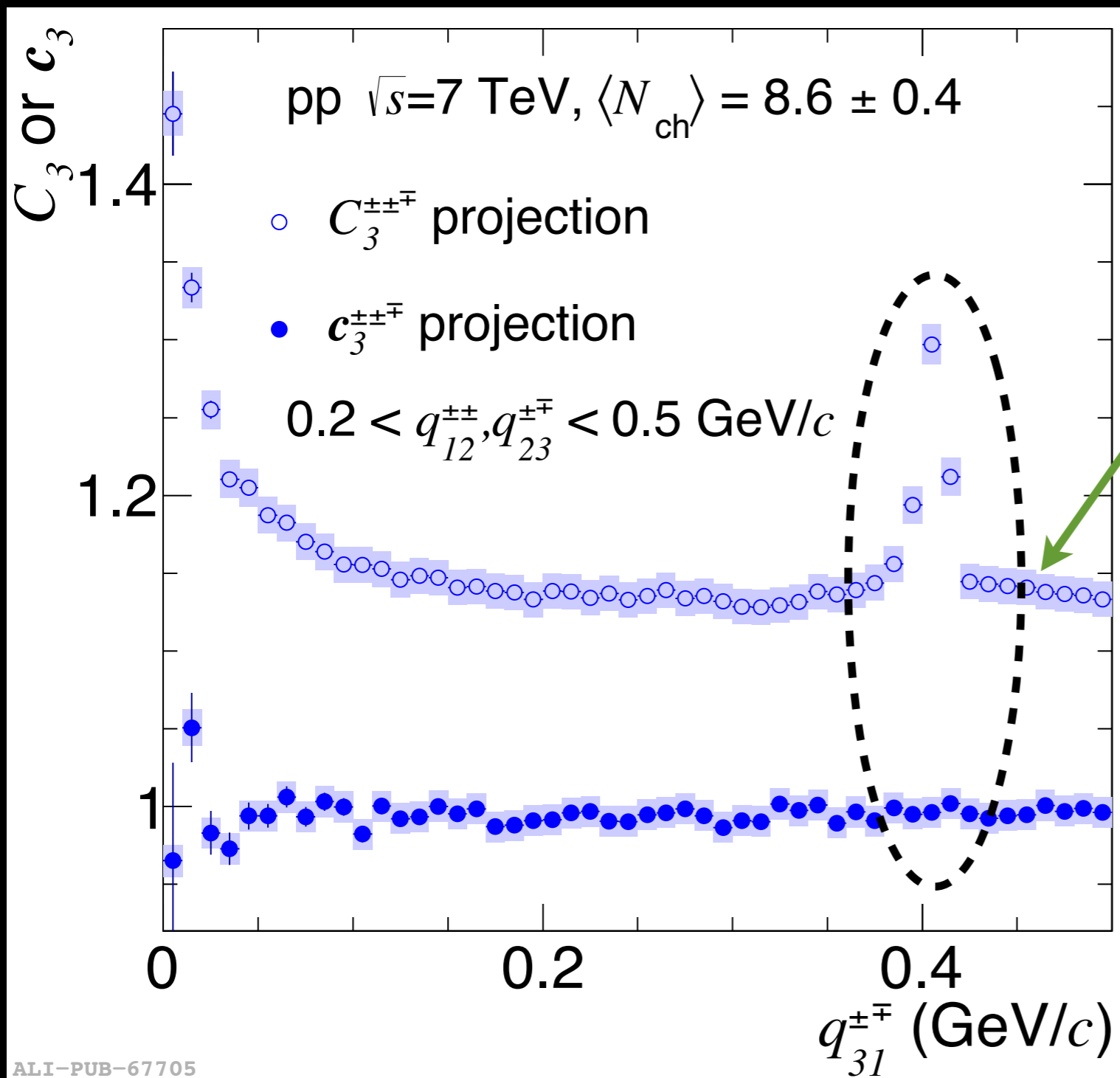
Pair Cuts

- Track merging and splitting:
pair angular separation

- For 3 (4) pions, pair cuts applied to all 3 (6) pairs in the triplet (quadruplet).

Freeze-out Radii
Extracted from 3-pion
Bose-Einstein Cumulants

3-pion cumulants remove 2-pion correlations

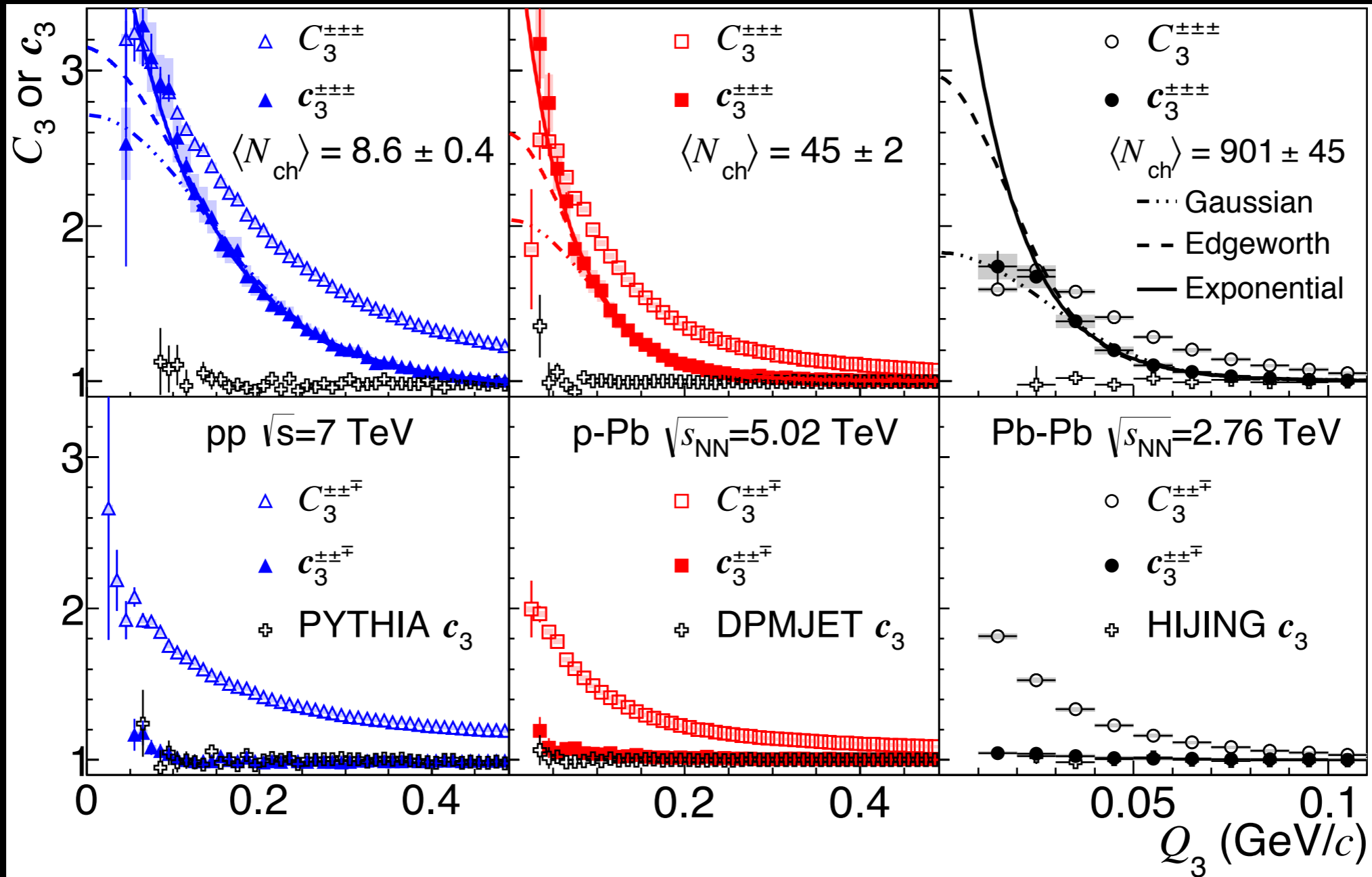


Hollow points:
 K^0_s peak visible.

Solid points:
 Cumulant.
 K^0_s peak removed

3-pion Correlation Functions

Same Charge



Mixed Charge

pp
low multiplicity

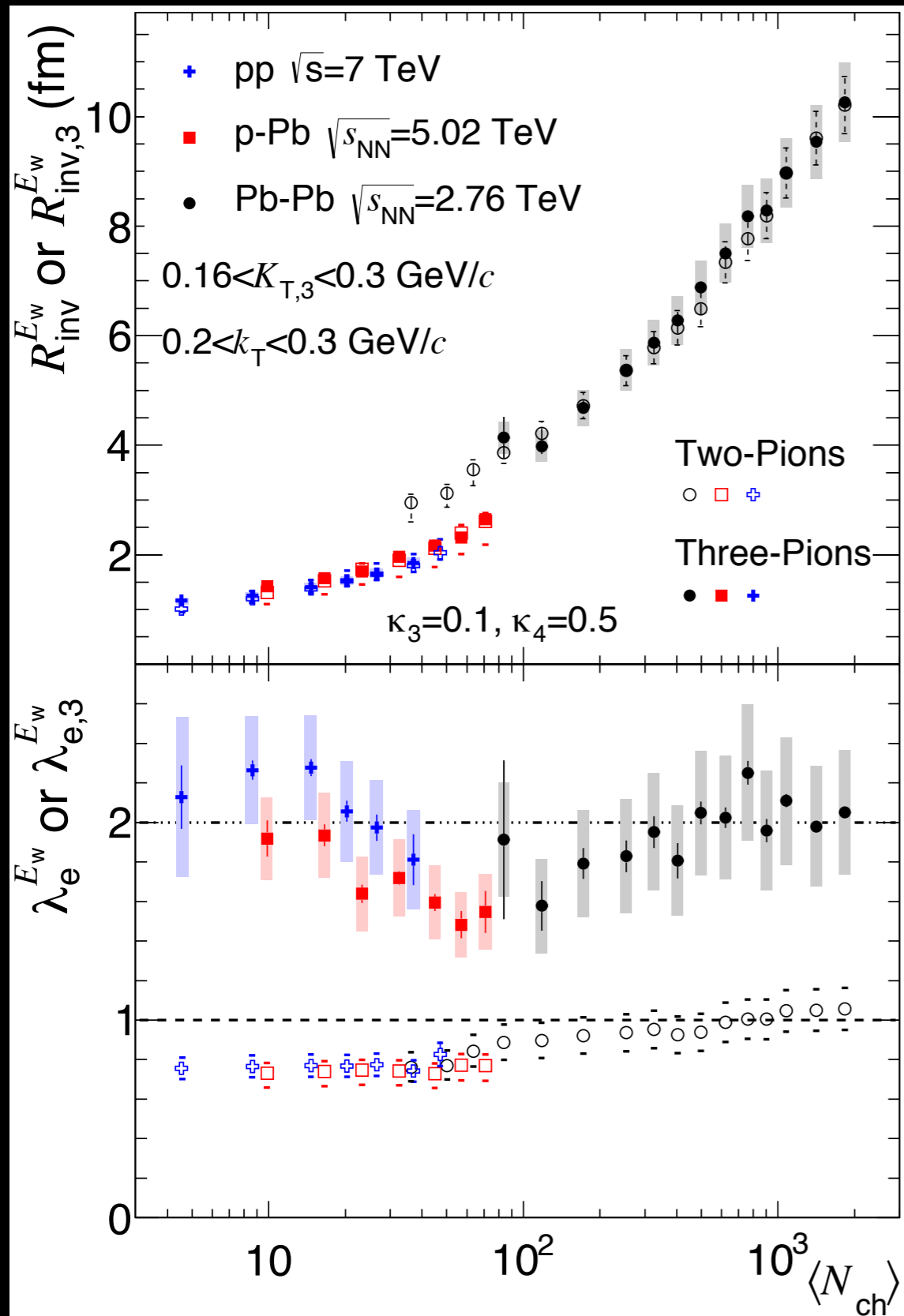
p-Pb
mid multiplicity

Pb-Pb
high multiplicity

ALICE

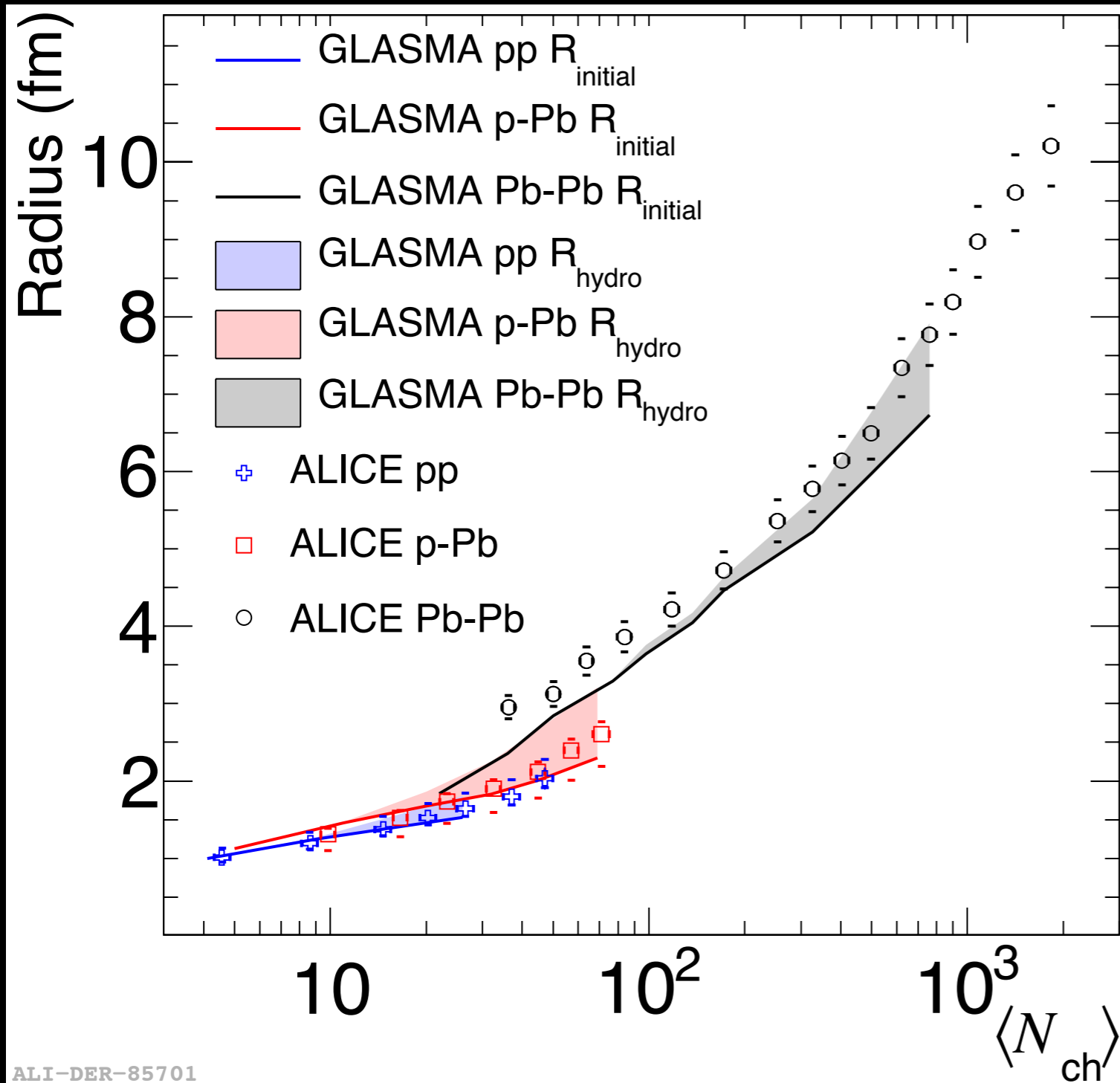
Phys. Lett. B accepted
arXiv:1404.1194 (2014)

Edgeworth Radii and Intercepts



- Non-Gaussian fits (Edgeworth or Exponential) provide a better fit of the correlation function.
- Radii report the 2nd cumulant of the Edgeworth correlation function.
- p-Pb similar to pp.
- Pb-Pb not similar to pp/p-Pb.
- Intercept parameters much closer to their chaotic limits.

Radii Comparison with IP-GLASMA



Message:

Similarity of ALICE radii in p-Pb and pp can be reproduced with GLASMA initial conditions alone.

They can also be reproduced with a hydrodynamic phase in p-Pb.

Schenke & Venugopalan
arXiv:1405.3605

- GLASMA points are first scaled such that the calculations in pp match the ALICE pp data. Scale = 1.15. GLASMA calculations have uncertainty due to infrared cutoff ($m=0.1$ GeV).

Coherence Measurements from 3-pion Cumulants

r_3

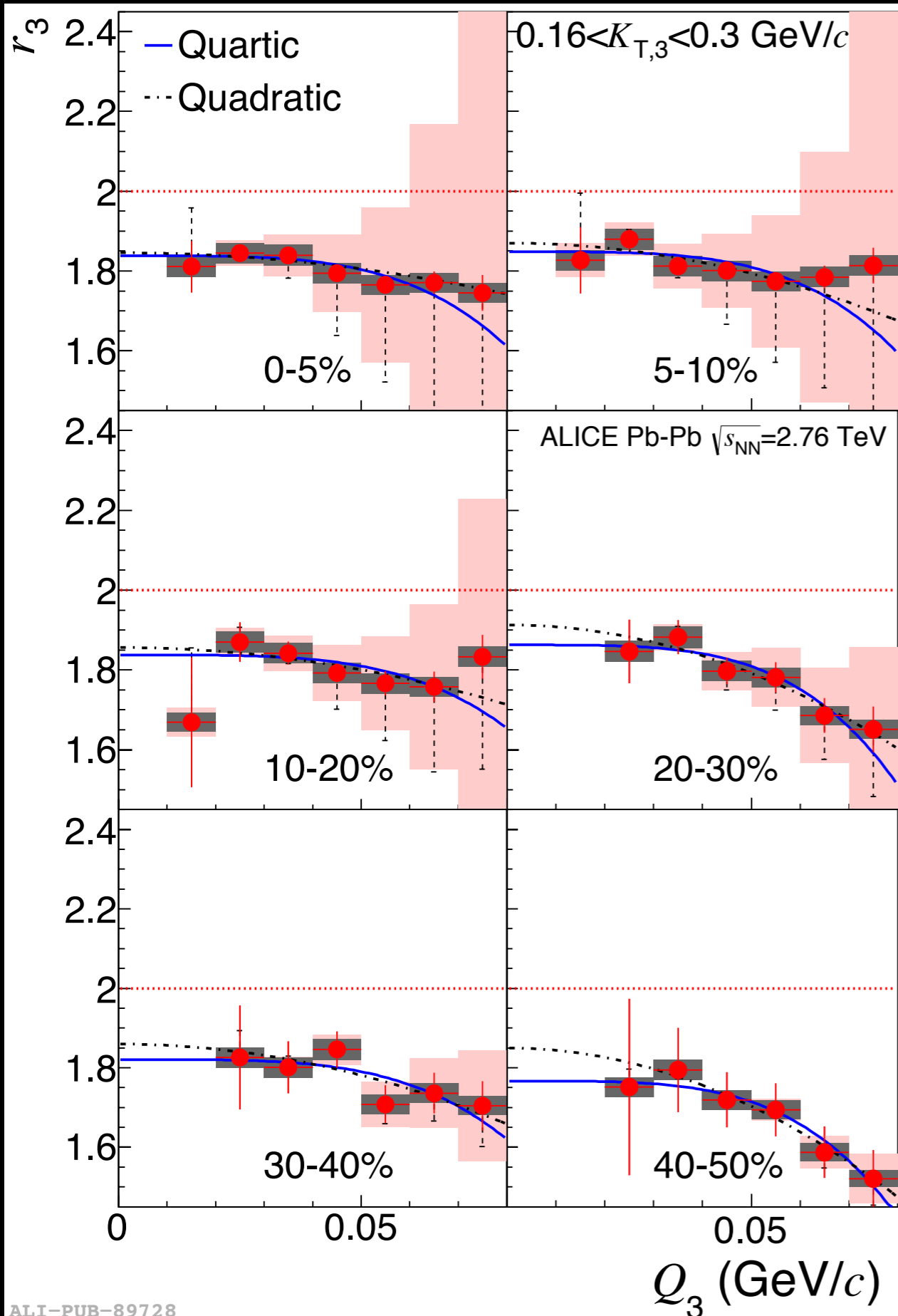
A comparison of 3-pion to 2-pion
Bose-Einstein correlation strengths

$$r_3(Q_3) = \frac{c_3(q_{12}, q_{23}, q_{31}) - 1}{\sqrt{(C_2(q_{12}) - 1)(C_2(q_{13}) - 1)(C_2(q_{23}) - 1)}}$$

$r_3(0) = 2.0$ for no coherence

$r_3(Q_3) = 2.0$ additionally for no 3-pion phase

r_3 for 6 centrality bins in Pb-Pb



$$r_3(Q_3) = \frac{c_3(q_{12}, q_{23}, q_{31}) - 1}{\sqrt{(C_2(q_{12}) - 1)(C_2(q_{13}) - 1)(C_2(q_{23}) - 1)}}$$

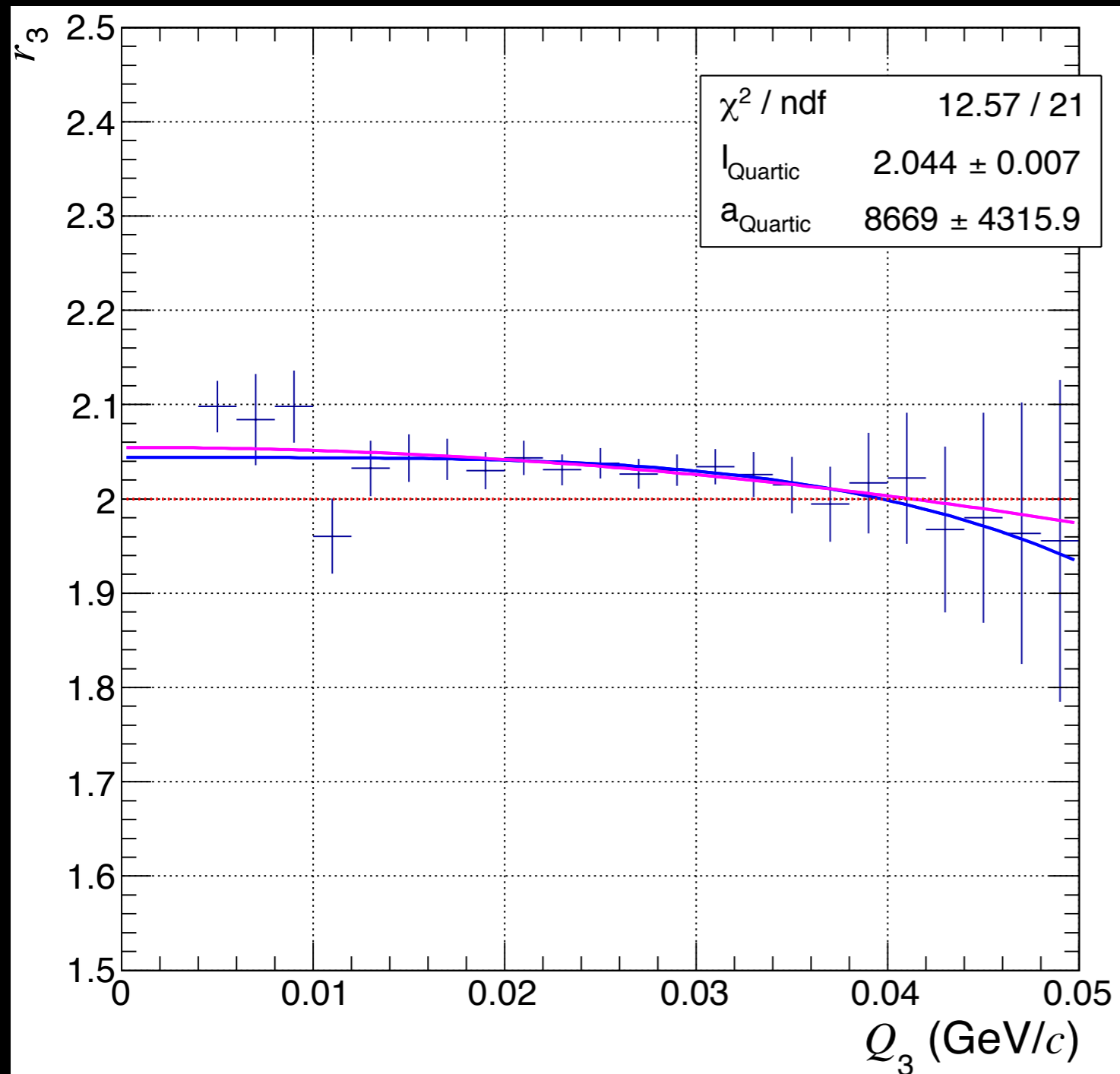
All correlations are first Coulomb corrected.

r_3 is suppressed below 2.0. Intercept corresponds to **23% \pm 8% coherence at low p_T .**

ALICE

PRC 89 024911 (2014)

r_3 Calculation in Therminator



Therminator model calculation without coherence.

No Q_3 dependence in this model.
= No effect of the 3-pion phase.

Therminator 2 model:
Kisiel et al.,
Comput. Phys. Commun. 174, 669
(2006)

Coherence Measurements from 4-pion Correlations

Equations to Build QS correlations with coherence

G = coherent fraction of pions

$$C_2^{QS} - 1 = (1 - G^2)T_{12}^2 \quad \text{Extract building block, } T_{ij}, \text{ from here} \quad (52)$$

$$C_3^{QS} - 1 = (1 - G)^2(T_{12}^2 + T_{13}^2 + T_{23}^2) \quad (53)$$

$$+ (6G(1 - G)^2 + 2(1 - G)^3)T_{12}T_{13}T_{23} \quad (54)$$

$$C_4^{QS} - 1 = (1 - G^2)(T_{12}^2 + T_{13}^2 + T_{14}^2 + T_{23}^2 + T_{24}^2 + T_{34}^2) \quad (55)$$

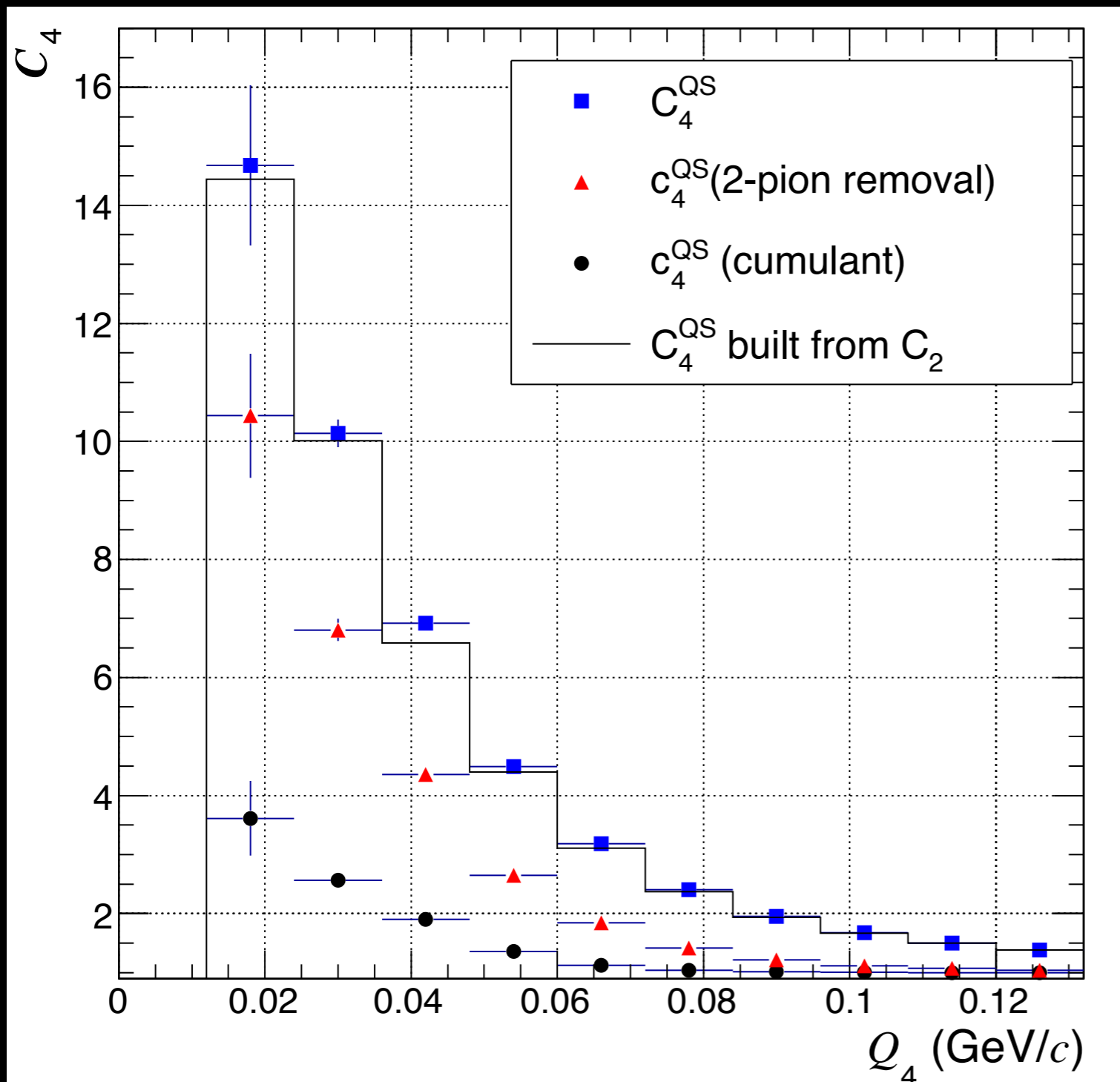
$$+ (4G(1 - G)^3 + (1 - G)^4(T_{12}^2T_{34}^2 + T_{13}^2T_{24}^2 + T_{14}^2T_{23}^2)) \quad (56)$$

$$+ (6G(1 - G)^2 + 2(1 - G)^3)(T_{12}T_{13}T_{23} + T_{12}T_{14}T_{24} + T_{13}T_{14}T_{34} + T_{23}T_{24}T_{34}) \quad (57)$$

$$+ (8G(1 - G)^3 + 2(1 - G)^4)(T_{12}T_{13}T_{24}T_{34} + T_{12}T_{14}T_{23}T_{34} + T_{13}T_{14}T_{23}T_{24}) \quad (58)$$

These equations valid for $R_{coh}=R_{ch}$ (coherent Radius = chaotic Radius).
We will also consider $R_{coh}=0$ (point source).

Proof of Principle

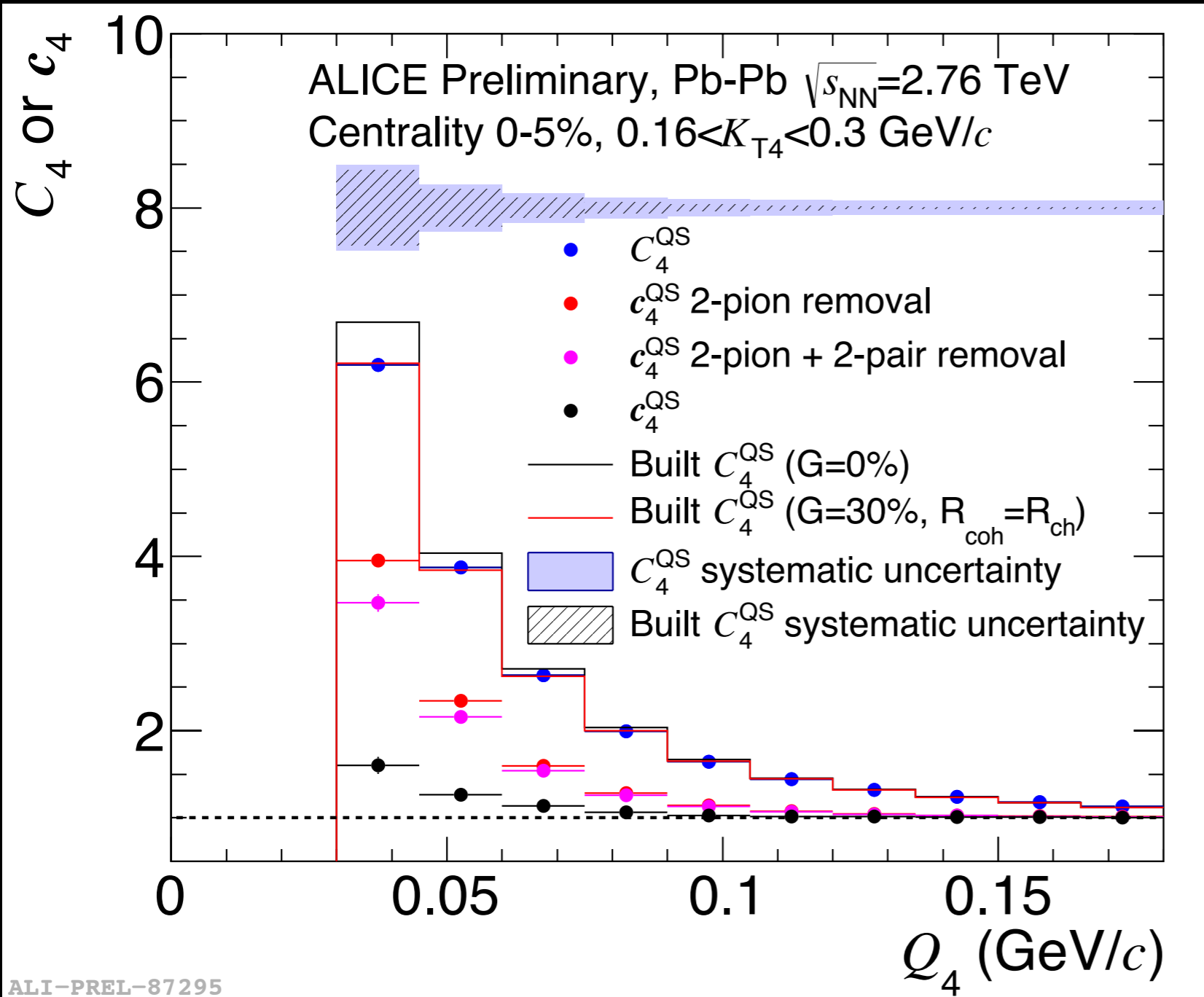
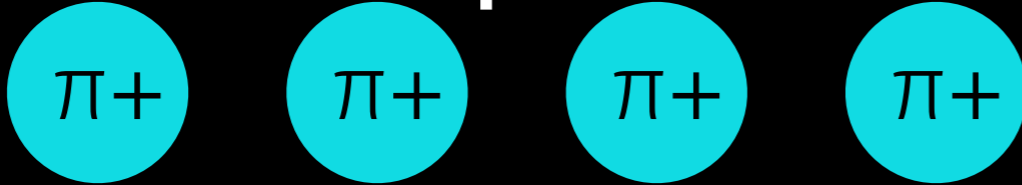


Therminator model calculation without coherence.

Measured 4-pion correlation is close to the “built” correlation.

Therminator 2 model:
Kisiel et al.,
Comput. Phys. Commun. 174, 669
(2006)

New: 4-pion Bose-Einstein



Extracted coherent fractions are again non-zero:
 $\sim 30\%$ for $R_{coh} = R_{ch}$
 $\sim 15\%$ for $R_{coh} = 0$

The Goal with Coherence Studies

We need a consistent picture from the comparison of all available orders of Bose-Einstein correlations:

3-to-2 (**done**)

4-to-2 (**done**)

4-to-3 (**ongoing**)

Consistent coherent fractions from each type makes a convincing case!

Work is ongoing to extract coherent fractions in pp and p-Pb.

Summary

Use
1

Freeze-out Radii:

- We have extracted freeze-out radii from 3-pion Bose-Einstein cumulants in pp, p-Pb, and Pb-Pb collisions.
- Radii in pp and p-Pb are quite similar, at similar multiplicity.
- Radii in Pb-Pb are quite different from pp and p-Pb, at similar multiplicity.
- Radii are consistent with initial conditions alone without a hydrodynamic phase. However, they do not rule out hydrodynamic expansion in all 3 systems.

Summary

Use
2

Quantum Coherence at Freeze-out:

- Our results indicate that 15-30% of charged pions may be coherent at freeze-out.
- First seen with the 3-to-2 comparison (r_3).
- Confirmed with the 4-to-2 comparison.
- Ongoing work to check 4-to-3 comparison.
- Ongoing work to extract coherent fractions in pp and p-Pb.

Survival of partial coherence would imply:

→ 2 disjunct particle-emitting sources!

→ Local thermal equilibrium at most.

→ Hydrodynamics not applicable to entire system of low p_T pions?

Supporting ALICE Publications

“Two- and three-pion quantum statistics correlations in Pb-Pb collisions at $\sqrt{s_{NN}} = 2.76$ TeV at the CERN Large Hadron Collider”

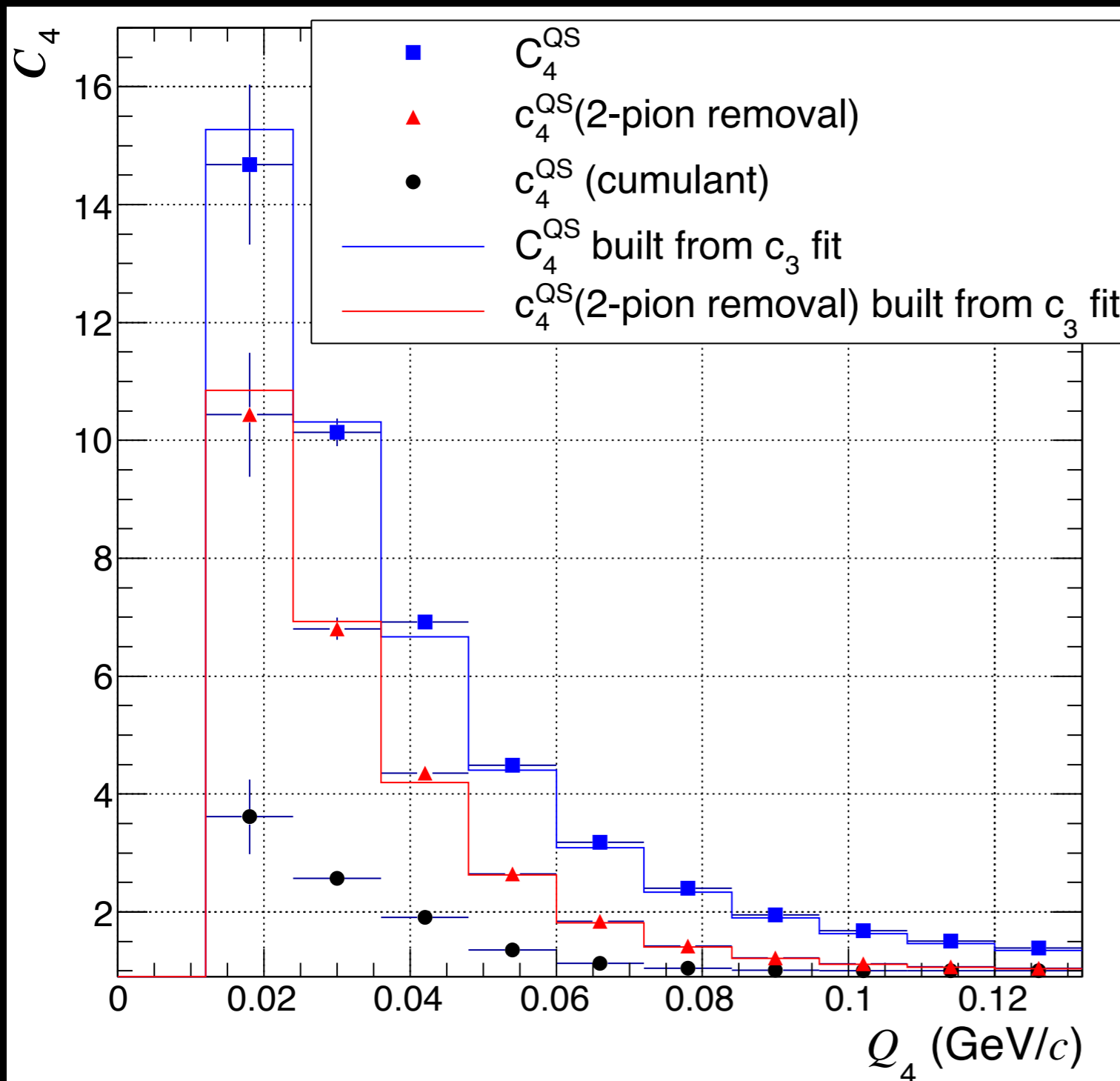
Phys. Rev. C **89** 024911 (2014)

“Freeze-out radii extracted from three-pion cumulants in pp, p-Pb and Pb-Pb collisions at the LHC”

Accepted by Phys. Lett. B. arXiv: 1404.1194 (2014)

Supporting Slides

Proof of Principle for building C_4 from c_3 fits

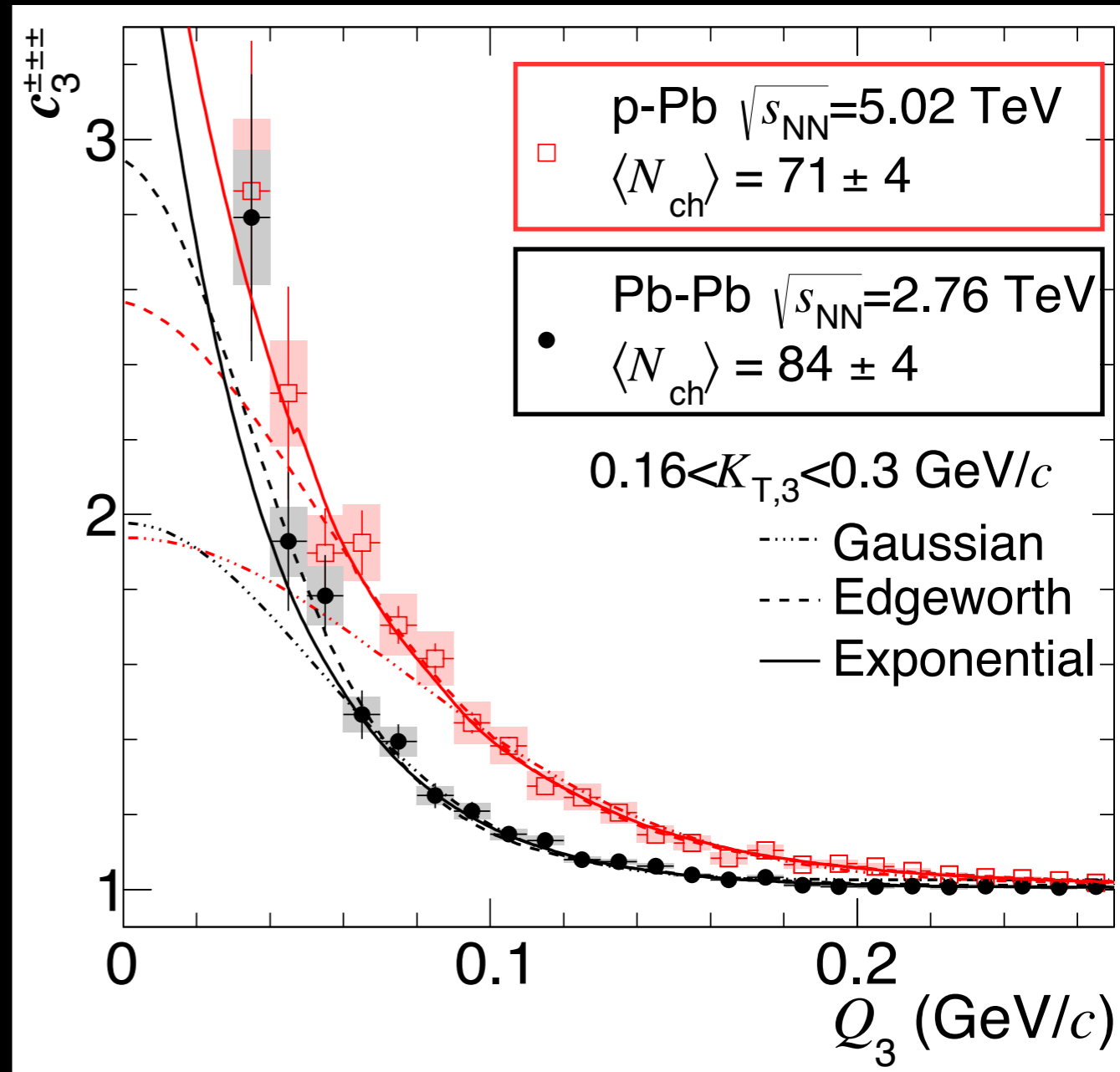
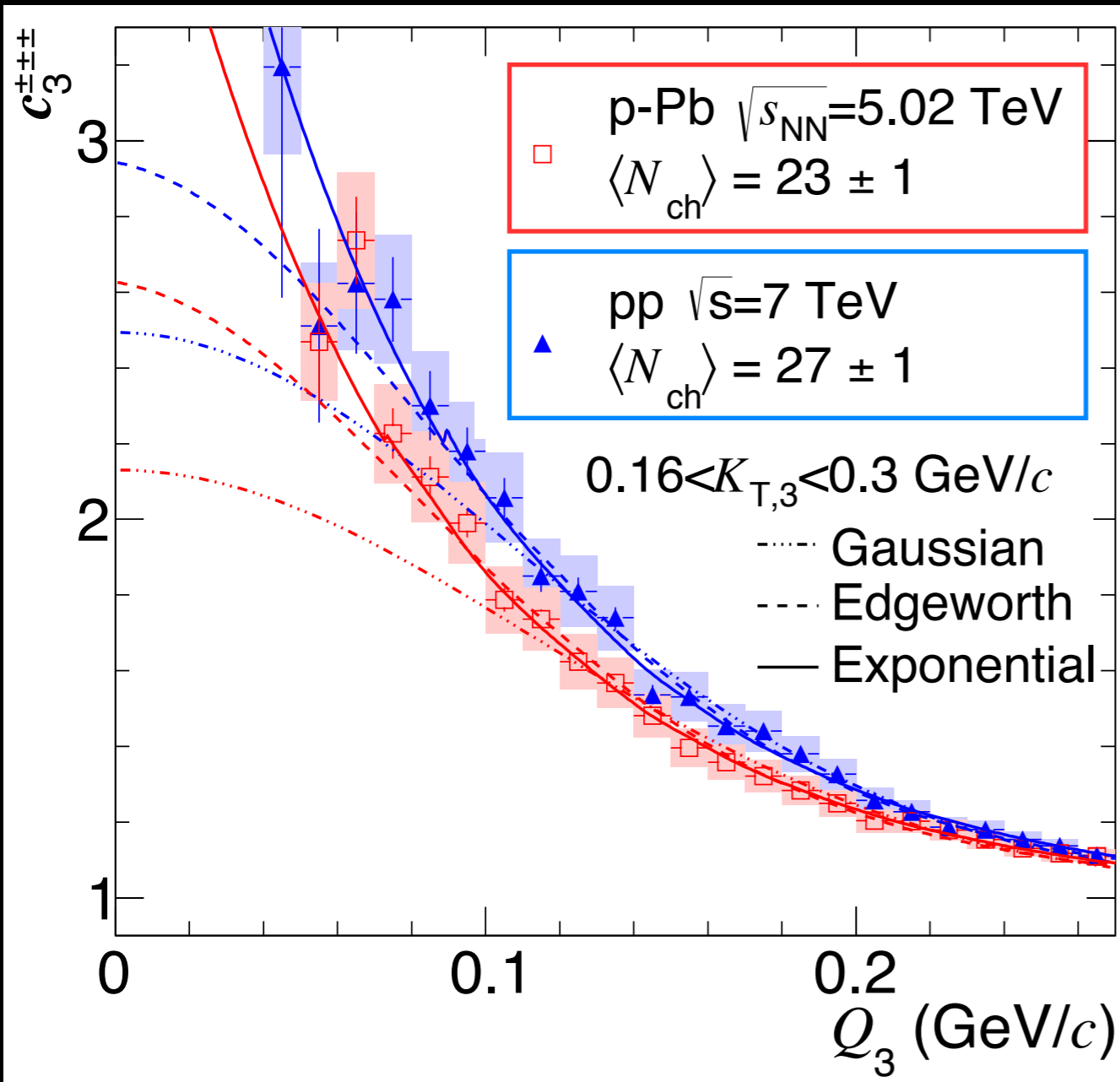


Therminator model calculation without coherence.

Measured C_4 and the partial cumulant c_4 (2-pion removal) are close to their "built" versions.

Therminator 2 model:
Kisiel et al.,
Comput. Phys. Commun. 174, 669
(2006)

Comparison of c_3 at similar N_{ch}



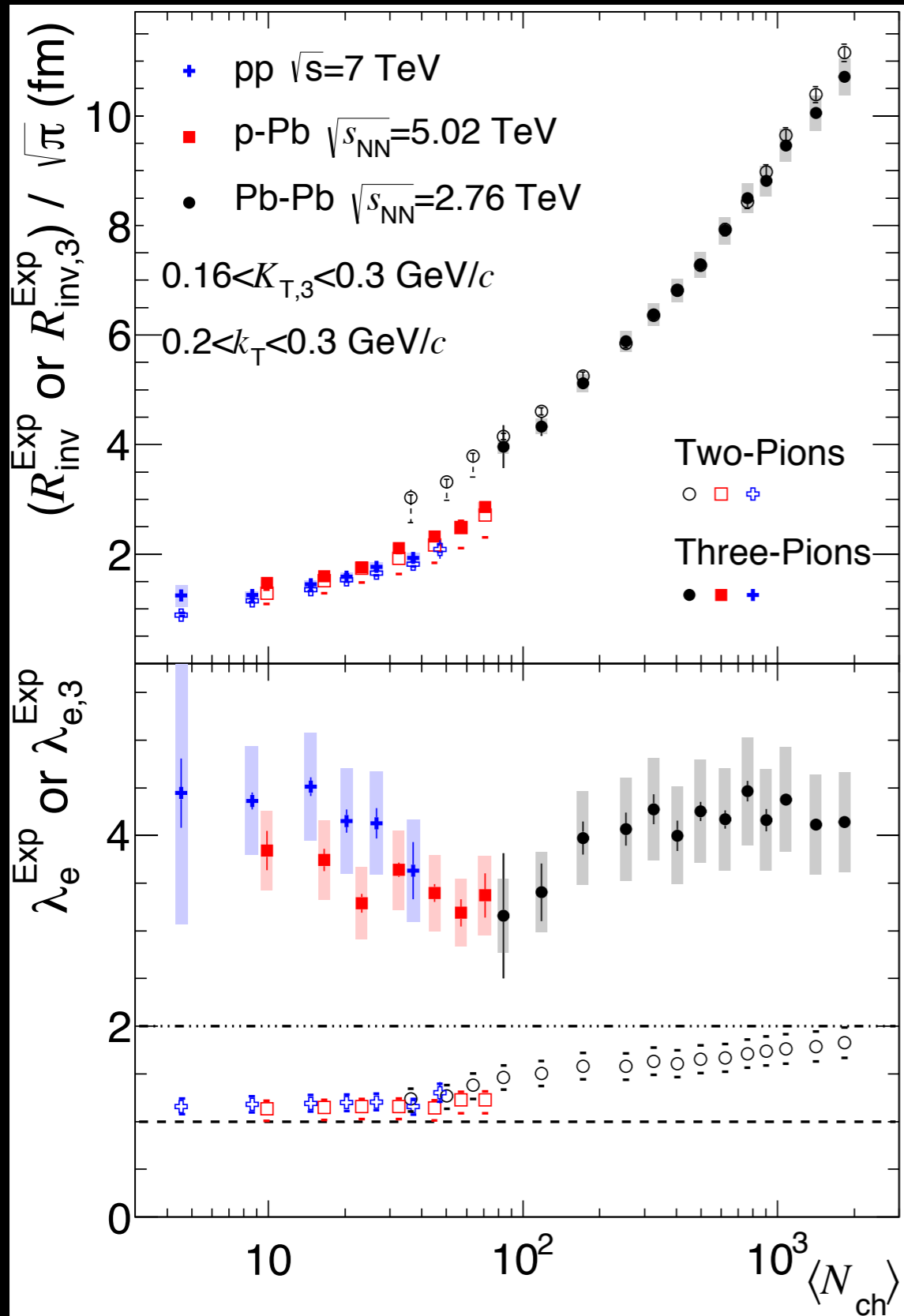
Correlation functions similar

Correlation functions different

ALICE

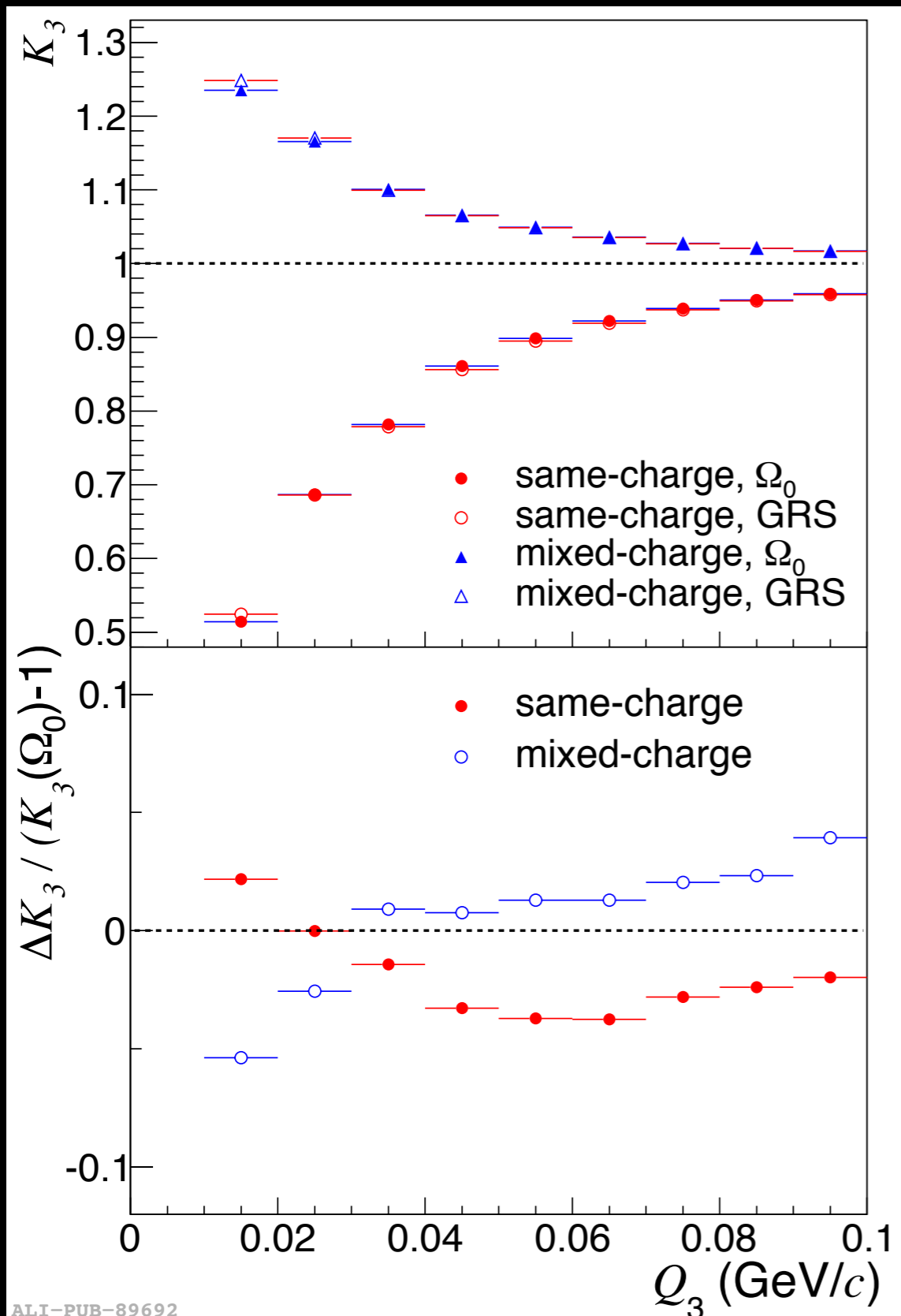
Phys. Lett. B accepted
arXiv:1404.1194 (2014)

Exponential Radii and Intercepts



- Exponential fits generally better fit low q part of the correlation function.
- Radii report FWHM of a Cauchy (Lorentzian) source profile.
- p-Pb similar to pp.
- Intercept parameters exceed the chaotic limits. Source profile cannot be entirely Cauchy.

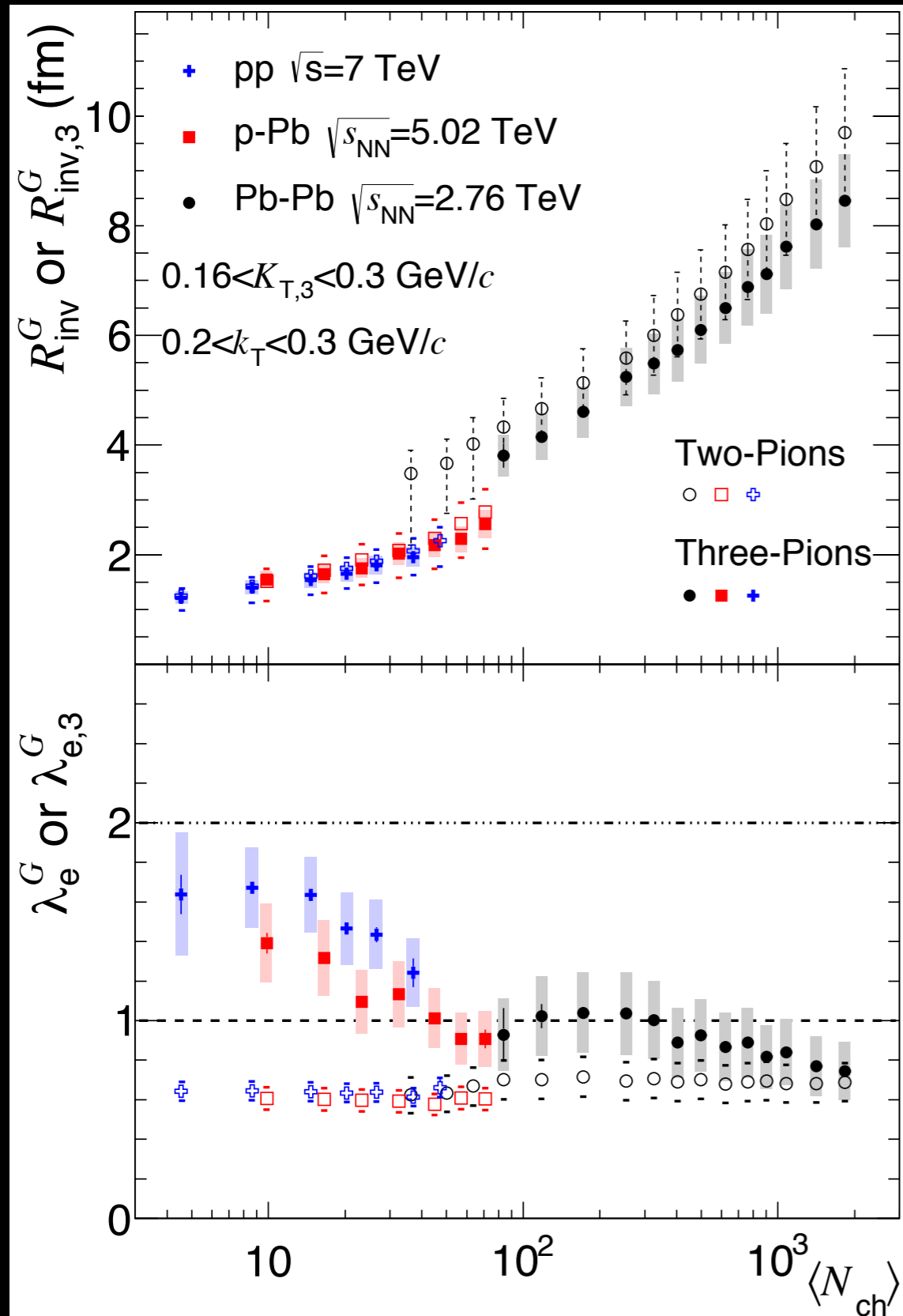
Near Equivalence between 2 types of Coulomb Calculations



Ω_0 = Full Asymptotic wave-function calculation.

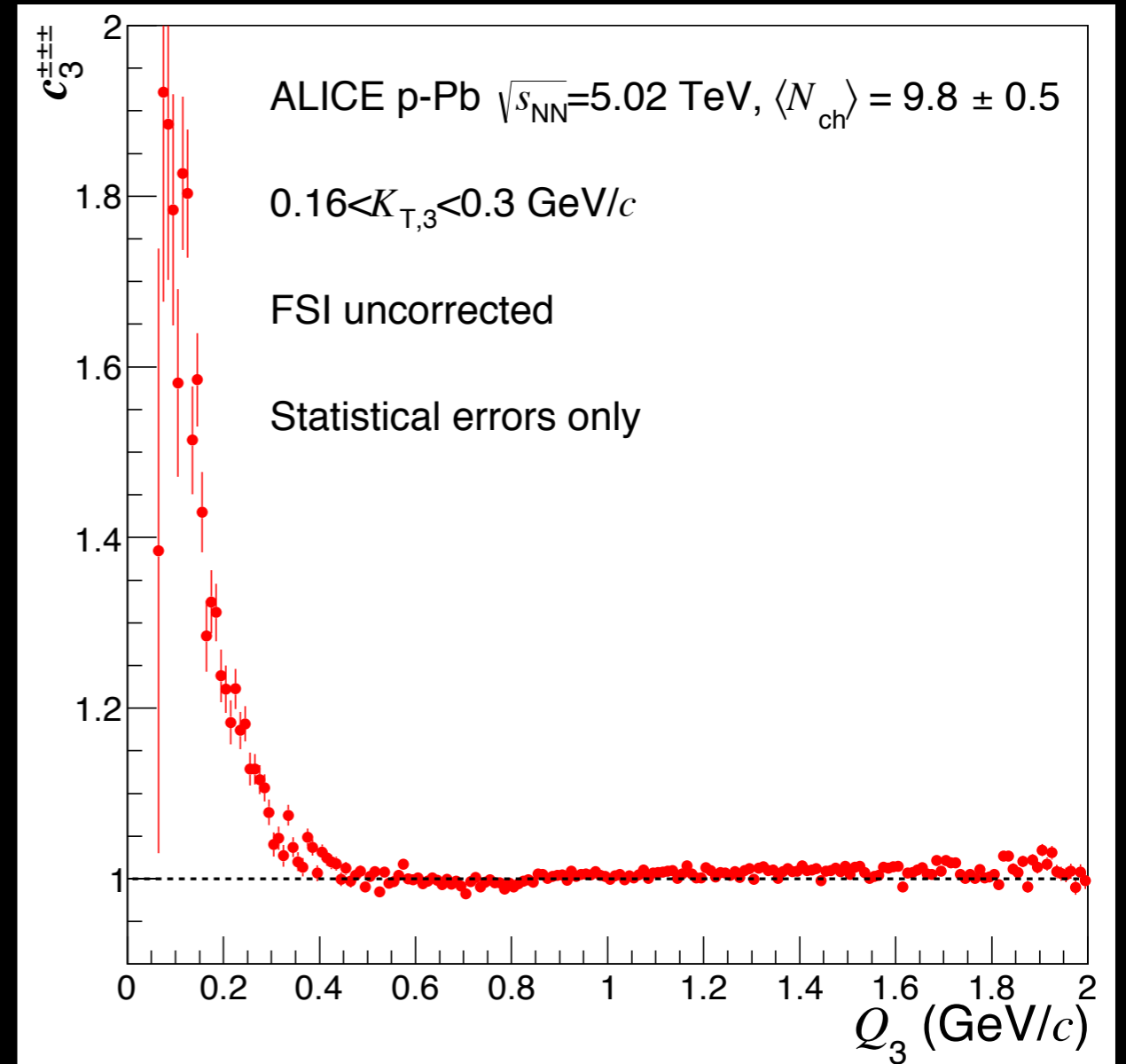
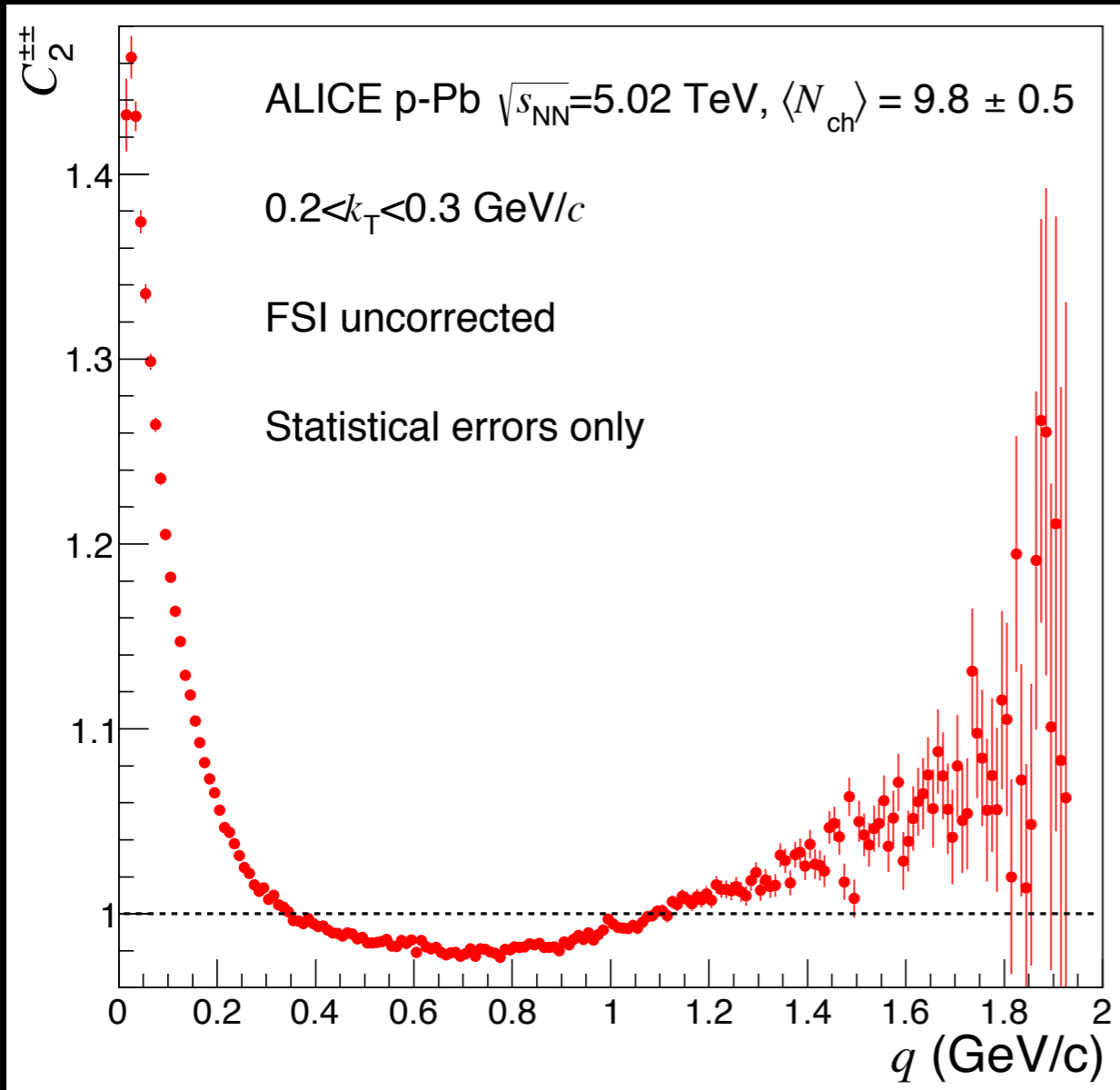
GRS = Generalized Riverside
= $K_{12}K_{13}K_{23}$

Gaussian Radii and Intercepts



- Gaussian fits were the worst at describing the correlation function.
- p-Pb similar to pp.
- Intercept parameters far below the chaotic limits. Source profile cannot be entirely Gaussian.

C_2 & c_3 in an extended range



The baseline for 3-pion cumulants is more flat than for 2-pion correlations.

2-boson Symmetrization

We consider 2 extreme cases for the size of the coherent source radius

Point source
 $R_{\text{coh}} = 0$

$$C_2(1, 2) = 1 + (1 - G)^2 (T_{12}^{\text{ch}})^2 + 2G(1 - G)T_{12}^{\text{ch}}$$

Full size source
 $R_{\text{coh}} = R_{\text{ch}}$

$$C_2(1, 2) = 1 + (1 - G)^2 (T_{12}^{\text{ch}})^2 + 2G(1 - G)(T_{12}^{\text{ch}})^2$$

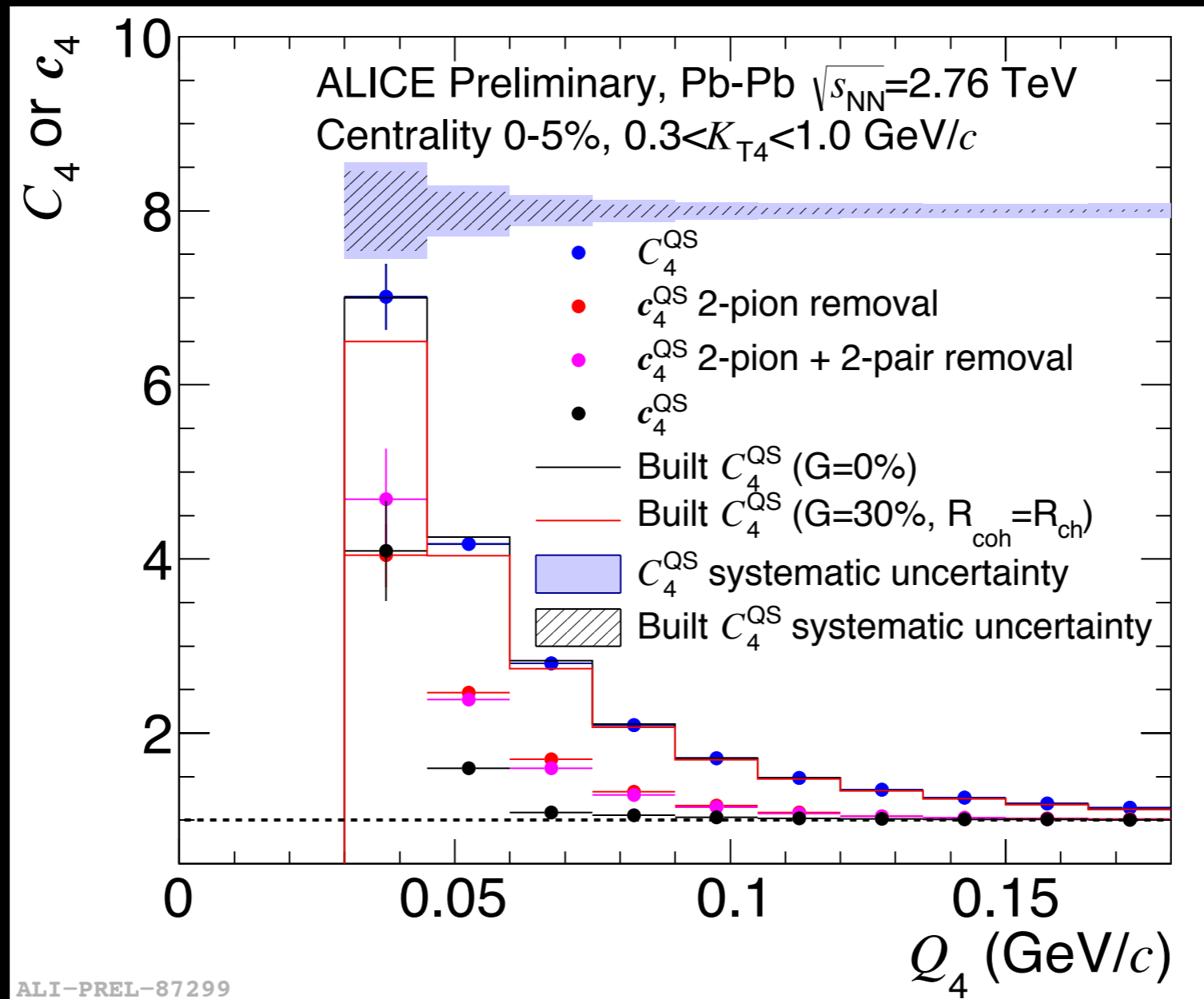
↑
Measured

↑
Assumed
value

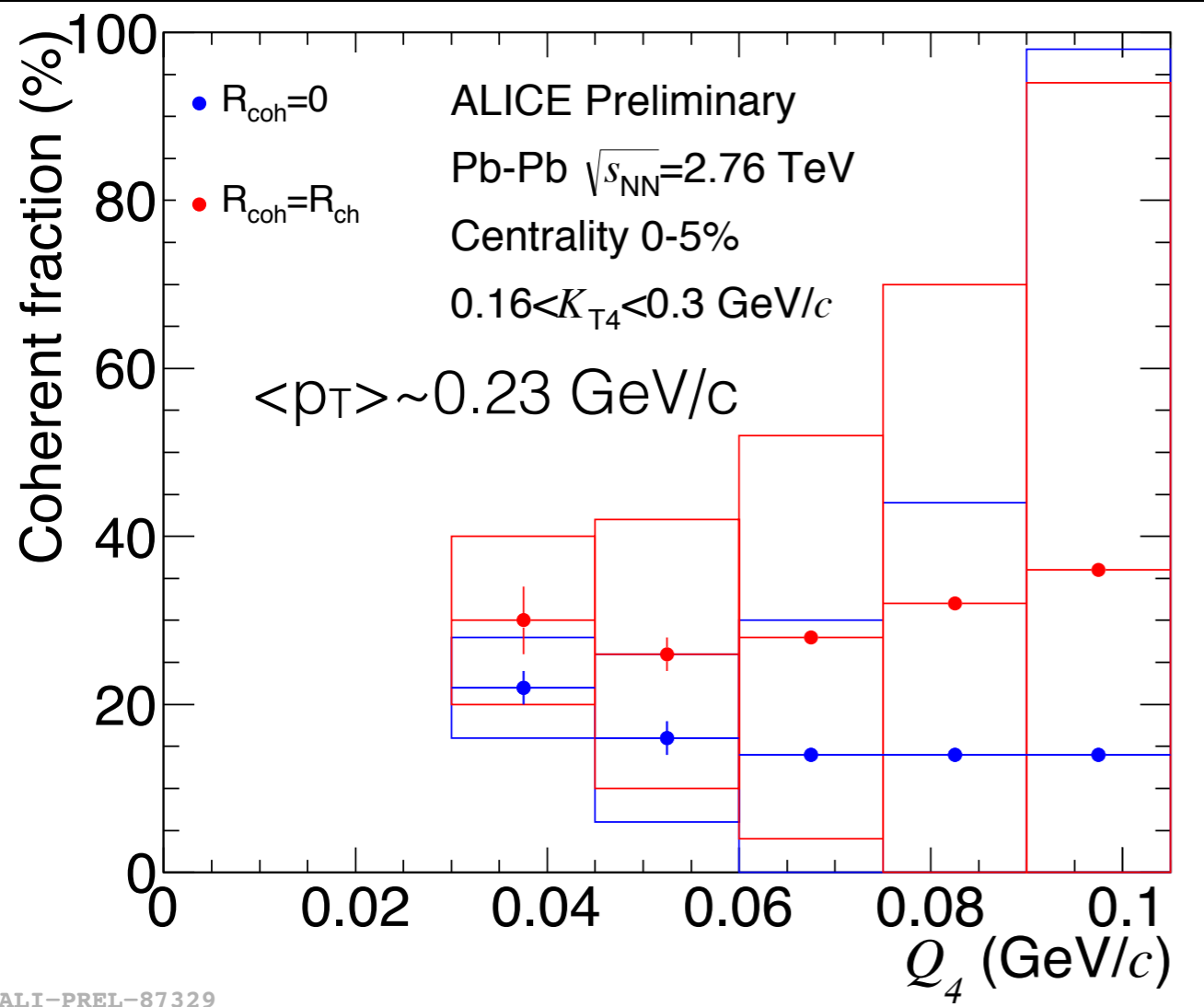
↑
Extracted

*Equations derived from
I. Andreev et al.
Int. J. Mod. Phys. A **8** 4577*

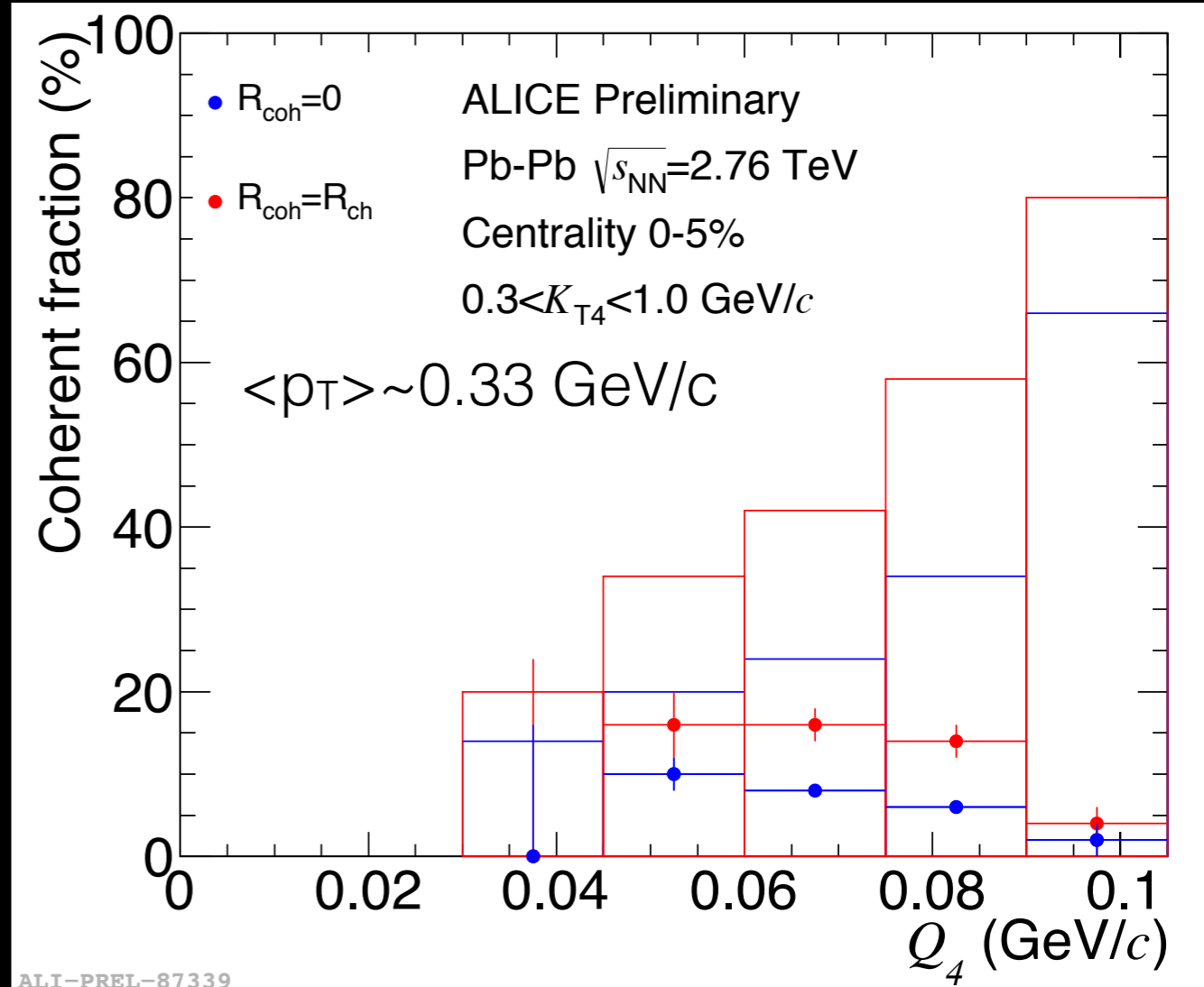
4-pion Bose-Einstein at High K_{T4}



Coherent Fractions vs. Q_4



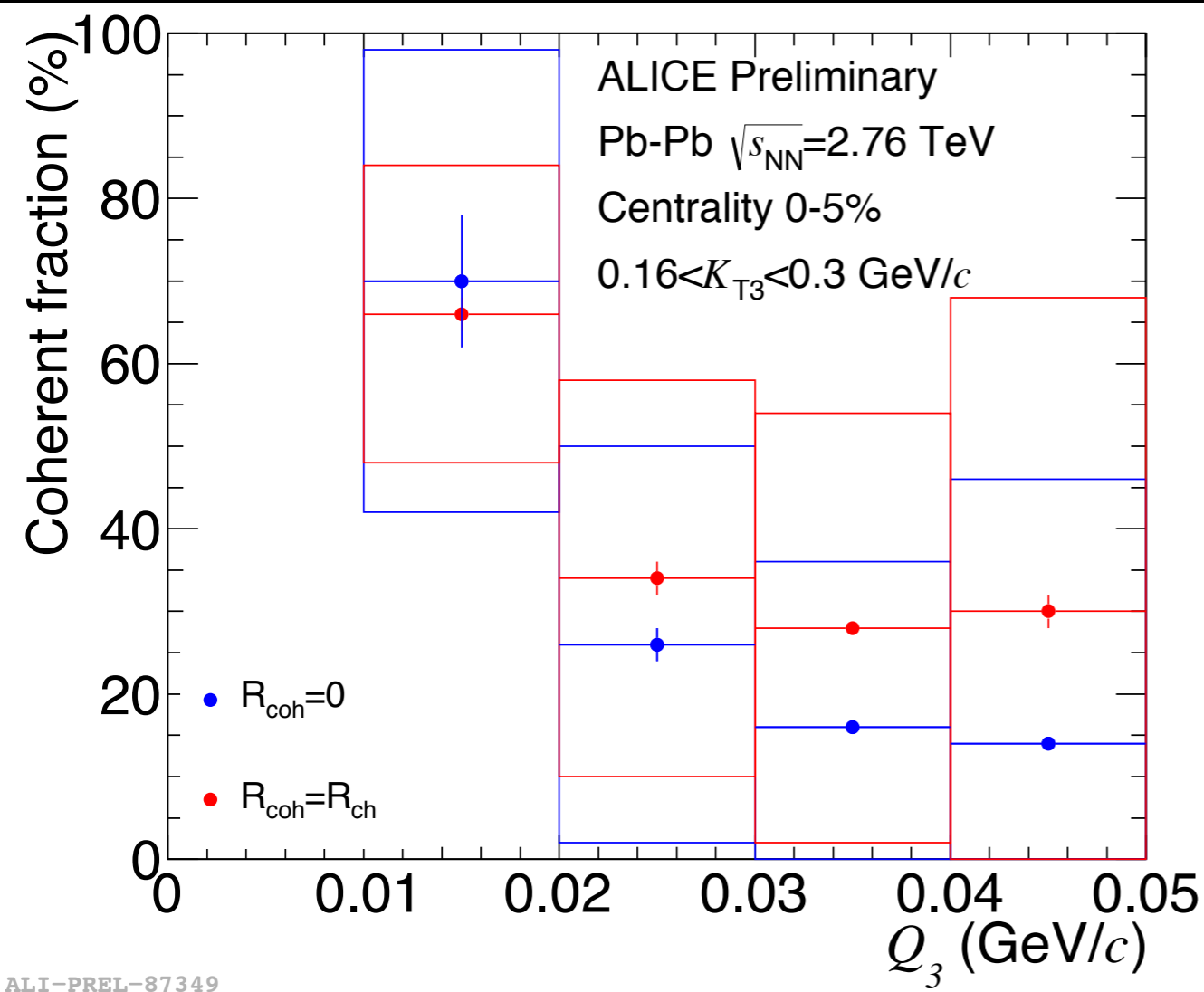
Low K_{T4}



High K_{T4}

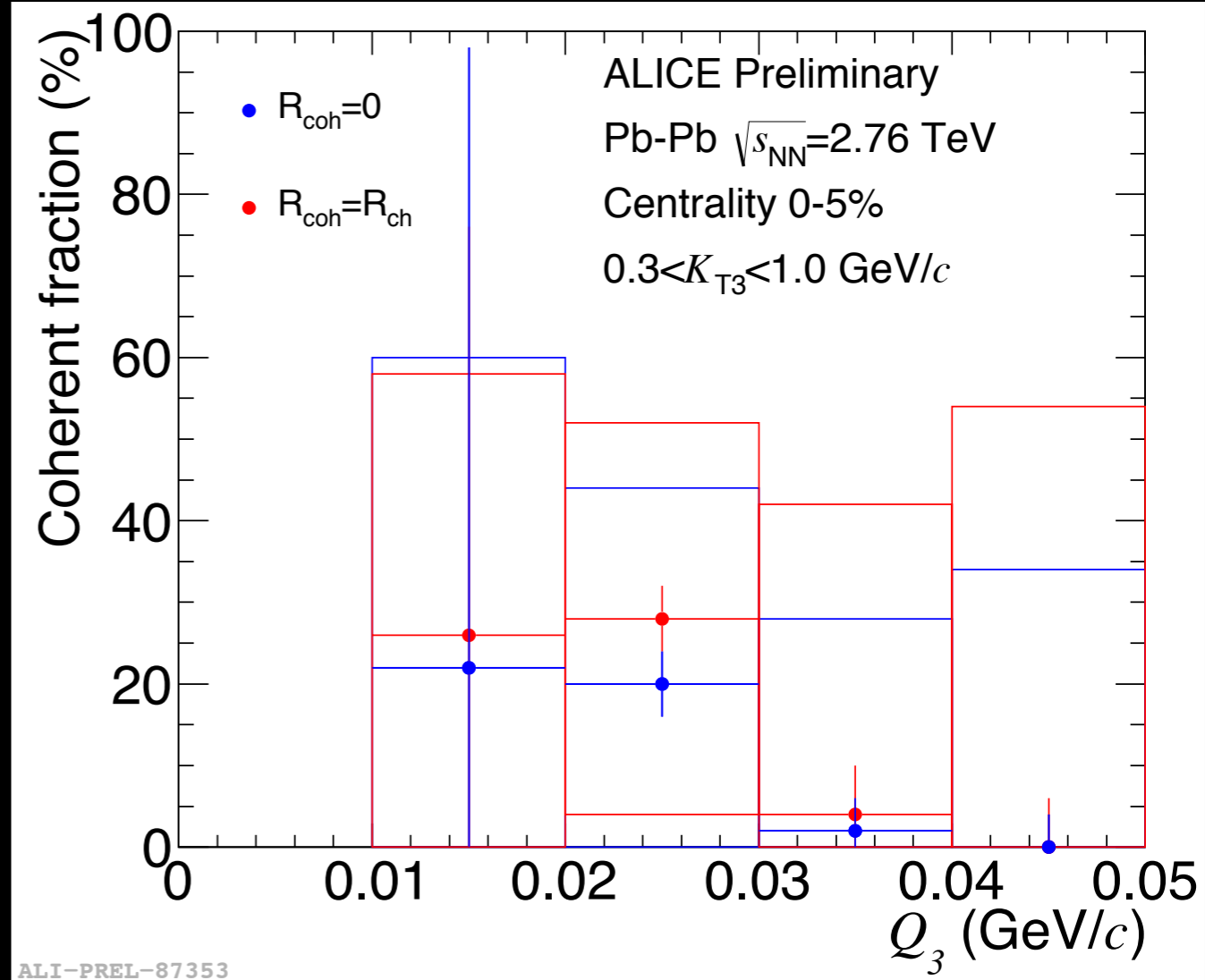
- Coherent fraction is fairly stable with Q_4 .
- Systematics dominated by - - - + residual correlation.

3-pions (C_3^{QS}) : Minima vs. Q_3



$\langle p_T \rangle \sim 0.23$ GeV/c

Low K_{T3}



$\langle p_T \rangle \sim 0.33$ GeV/c

High K_{T3}

- Coherent fraction is fairly stable with Q_4 .
- Systematics dominated by - - - + residual correlation.

Isolation of 2-pion Quantum Statistics (QS)

Quantity of Interest

$$N_2(p_1, p_2) = f_{21} N_1(p_1) N_1(p_2) + f_{22} K_2(q_{12}) N_2^{QS}(p_1, p_2)$$

Sinyukov et al.,
Phys. Lett. B 432, 249 (1998)

f_{22} estimated to be 0.7 ± 0.05 for this analysis

$$f_{21} = 1 - f_{22}$$

f_{22} previously estimated in
ALICE 2014
PRC 89 024911 (2014)

Isolation of 3-pion QS

ALICE 2014
PRC 89 024911 (2014)

Quantity of Interest



$$\begin{aligned} N_3(p_1, p_2, p_3) &= f_{31} N_1(p_1) N_1(p_2) N_1(p_3) \\ &+ f_{32} N_2(p_1, p_2) N_1(p_3) \\ &+ f_{33} K_3(q_{12}, q_{13}, q_{23}) N_3^{QS}(p_1, p_2, p_3) \end{aligned}$$

f coefficients derived in the core/halo picture as:

$$\begin{aligned} f_{31} &= (1 - f_c)^3 + 3f_c(1 - f_c)^2 - 3(1 - f_c)(1 - f_c^2) \\ f_{32} &= 3(1 - f_c) \\ f_{33} &= f_c^3 \end{aligned}$$

$f_c^2 = \text{“lambda”} = 0.7 \pm 0.05$ (fraction of correlated pairs)

Systematics Checked

Those which pertain to both measured and built C_4^{QS}

Systematics are Q_4 dependent

- - vs. + pions — 0.1%.
- TPC B field orientation — negligible.
- Tracking efficiency — 0.4% at low Q_4 .
- variation of f_c^2 (pair dilution). Default = 0.7, tried 0.65 and 0.75 — 6% at low Q_4
- Momentum resolution corrections — 1% at low Q_4
- Muon correction uncertainties — 2% at low Q_4 .

High degree of correlation between measured and built C_4^{QS} for each of these variations.

Systematics Checked

Measured C_4^{QS} only

Systematics are Q_4 dependent

- variation of $f_{41}, f_{42}, f_{43}, f_{44}$ from Therminator as compared to Core/Halo prescription — 0.4% at high Q_4
- Residue of mixed-charge (- - - +) cumulant — 5%
- K_4 FSI factor — 1% uncertainty at low Q_4 .
test of factorization: $K_4 = K_2^{12} K_2^{13} K_2^{14} K_2^{23} K_2^{24} K_2^{34}$

These systematics are the least understood sources of uncertainties. Future studies may reveal smaller values.

Systematics Checked

Built C_4^{QS} only

Systematics are Q_4 dependent

- Interpolator of 2-particle weights ($C_{2-1} = T_{ij}$) — 0.7% at low Q_4 . Cubic interpolation used in between bins of q_{out} , q_{side} , q_{long} by default. Linear interpolation used as a variation.
- 2-particle weight problem at high q_{inv}
Statistical fluctuations at high q_{inv} can give a negative T_{ij} which is not allowed in theory (Bose-Einstein correlations are positive). In these cases T_{ij} is set to zero.
 - 0.3% at high Q_4 , Low K_{T4}
 - 4% at high Q_4 , High K_{T4}

Equations to Build QS correlations with coherence, $R_{\text{coh}}=0$

$$C_2^{QS} - 1 = 2G(1-G)T_{12} + (1-G)^2 T_{12}^2$$

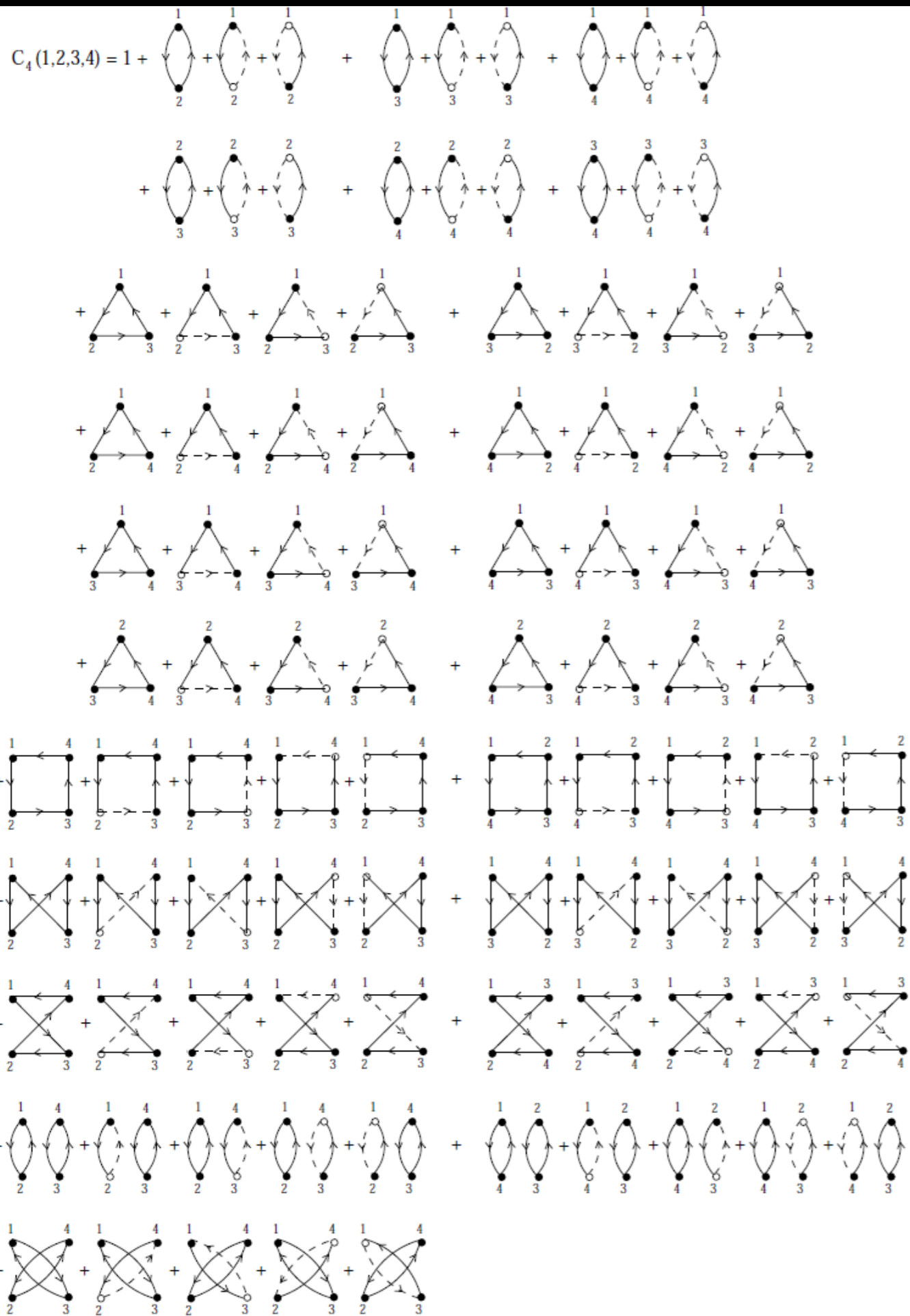
$$\begin{aligned}
 C_3^{QS} - 1 &= 2G(1-G)(T_{12} + T_{13} + T_{23}) + (1-G)^2(T_{12}^2 + T_{13}^2 + T_{23}^2) \\
 &+ 2G(1-G)^2(T_{12}T_{13} + T_{12}T_{23} + T_{13}T_{23}) + 2(1-G)^3(T_{12}T_{13}T_{23}) \\
 C_4^{QS} - 1 &= 2G(1-G)(T_{12} + T_{13} + T_{14} + T_{23} + T_{24} + T_{34}) \\
 &+ (1-G)^2(T_{12}^2 + T_{13}^2 + T_{14}^2 + T_{23}^2 + T_{24}^2 + T_{34}^2) \\
 &+ 2G(1-G)^3(T_{12}T_{34}^2 + T_{12}^2T_{34} + T_{13}T_{24}^2 + T_{13}^2T_{24} + T_{14}T_{23}^2 + T_{14}^2T_{23}) \\
 &+ (1-G)^4(T_{12}^2T_{34}^2 + T_{13}^2T_{24}^2 + T_{14}^2T_{23}^2) \\
 &+ 2G(1-G)^2(T_{12}T_{13} + T_{12}T_{23} + T_{13}T_{23} + T_{12}T_{14} + T_{12}T_{24} + T_{14}T_{24}) \\
 &+ 2G(1-G)^2(T_{13}T_{14} + T_{13}T_{34} + T_{14}T_{34} + T_{23}T_{24} + T_{23}T_{34} + T_{24}T_{34}) \\
 &+ 2(1-G)^3(T_{12}T_{13}T_{23} + T_{12}T_{14}T_{24} + T_{13}T_{14}T_{34} + T_{23}T_{24}T_{34}) \\
 &+ 2G(1-G)^3(T_{12}T_{14}T_{34} + T_{12}T_{14}T_{23} + T_{12}T_{23}T_{34} + T_{14}T_{23}T_{34}) \\
 &+ 2G(1-G)^3(T_{12}T_{13}T_{34} + T_{12}T_{34}T_{24} + T_{12}T_{24}T_{13} + T_{13}T_{24}T_{34}) \\
 &+ 2G(1-G)^3(T_{14}T_{13}T_{23} + T_{14}T_{13}T_{24} + T_{13}T_{23}T_{24} + T_{14}T_{24}T_{23}) \\
 &+ 2(1-G)^4(T_{12}T_{13}T_{24}T_{34} + T_{12}T_{14}T_{23}T_{34} + T_{13}T_{14}T_{23}T_{24})
 \end{aligned}$$

G = coherent fraction of pions

Weiner et al.
Int.J.Mod.Phys.A.
26 4577 (1993)

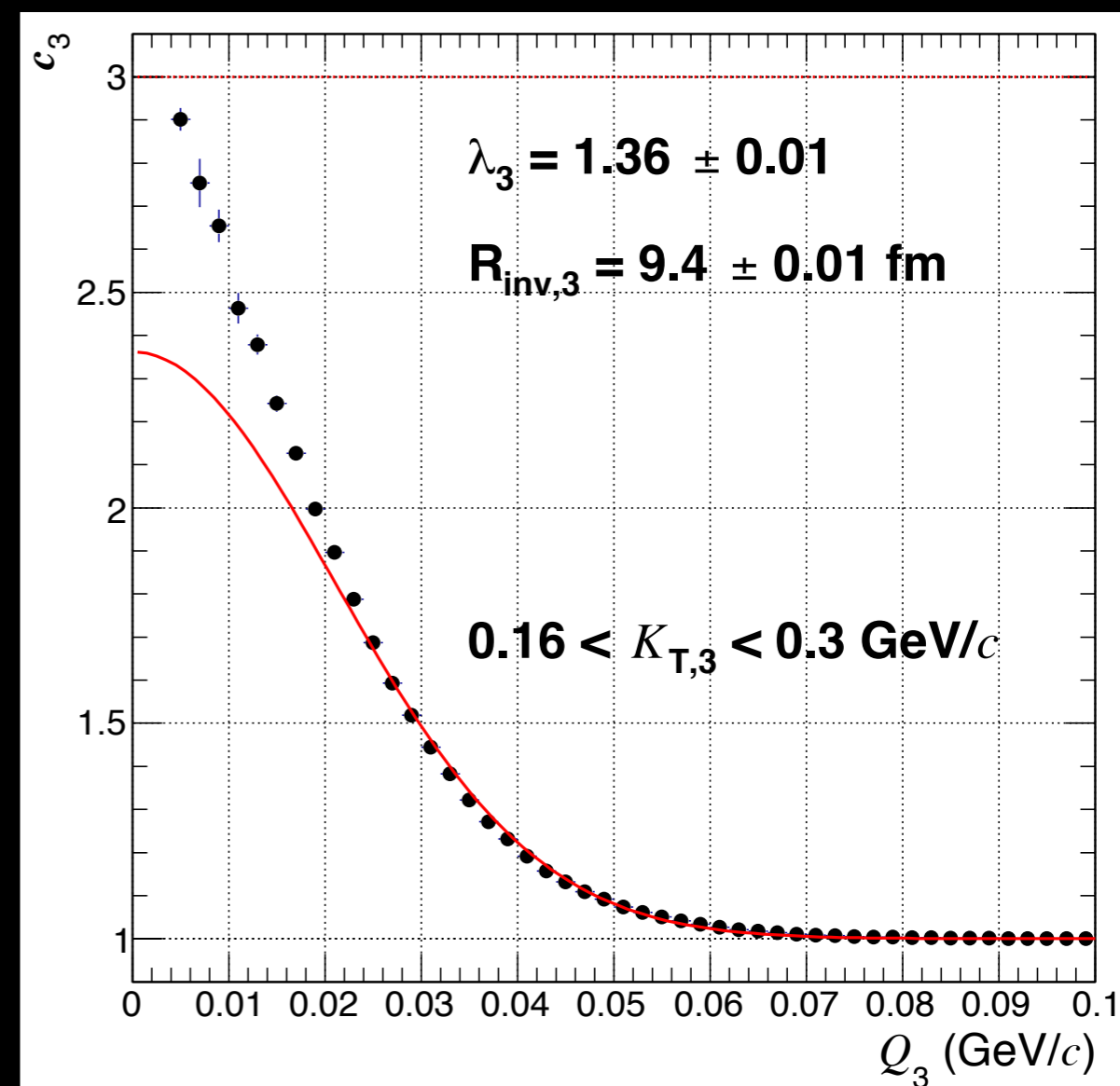
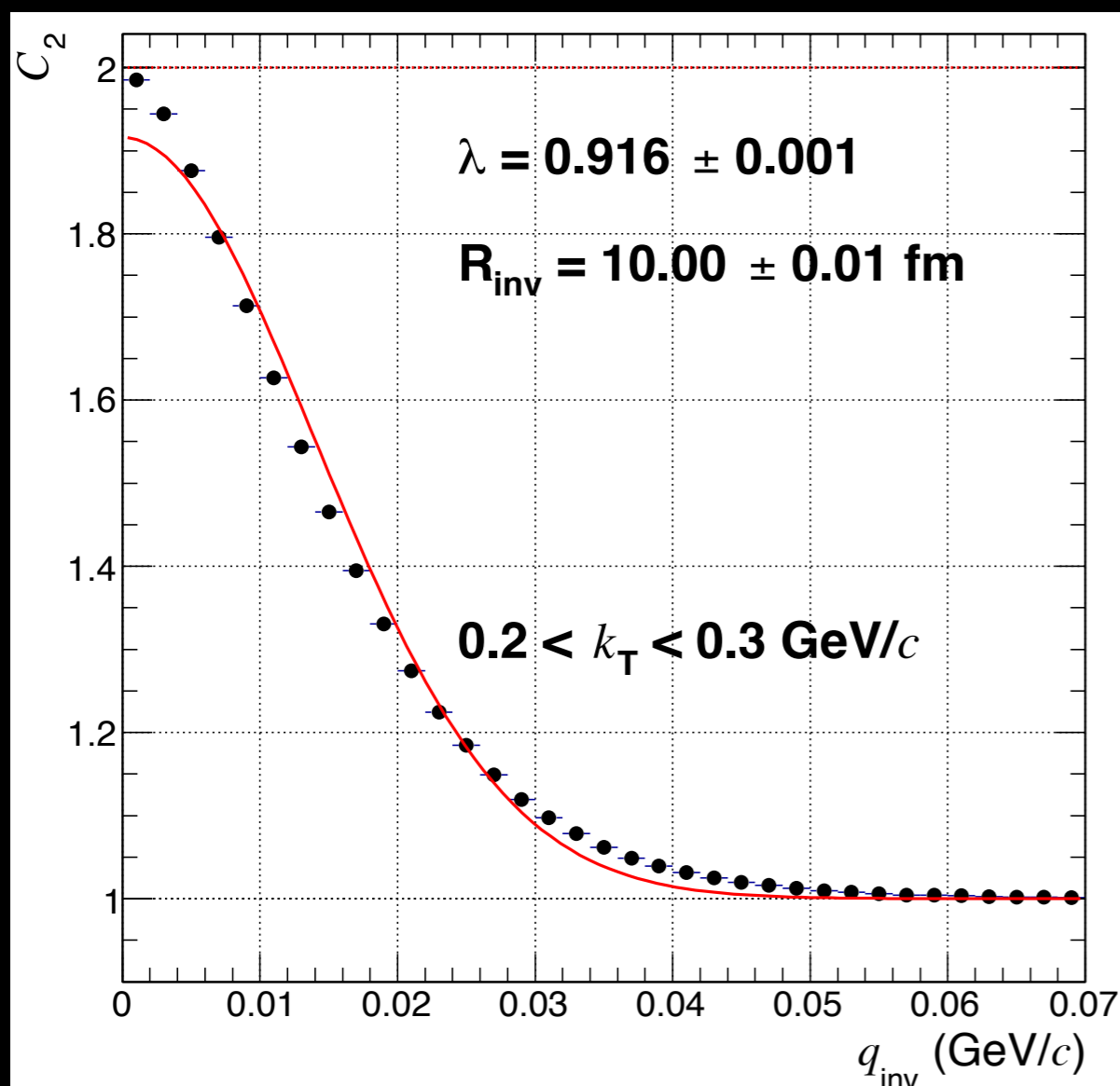
T. Csorgo.
Heavy Ion Phys.
15 1 (2002)

Full 4-pion Quantum Interference Diagrams



T. Csorgo
Heavy Ion Physics **15** 1-80

Therminator2 calculations of 2- and 3-pion Bose-Einstein correlations

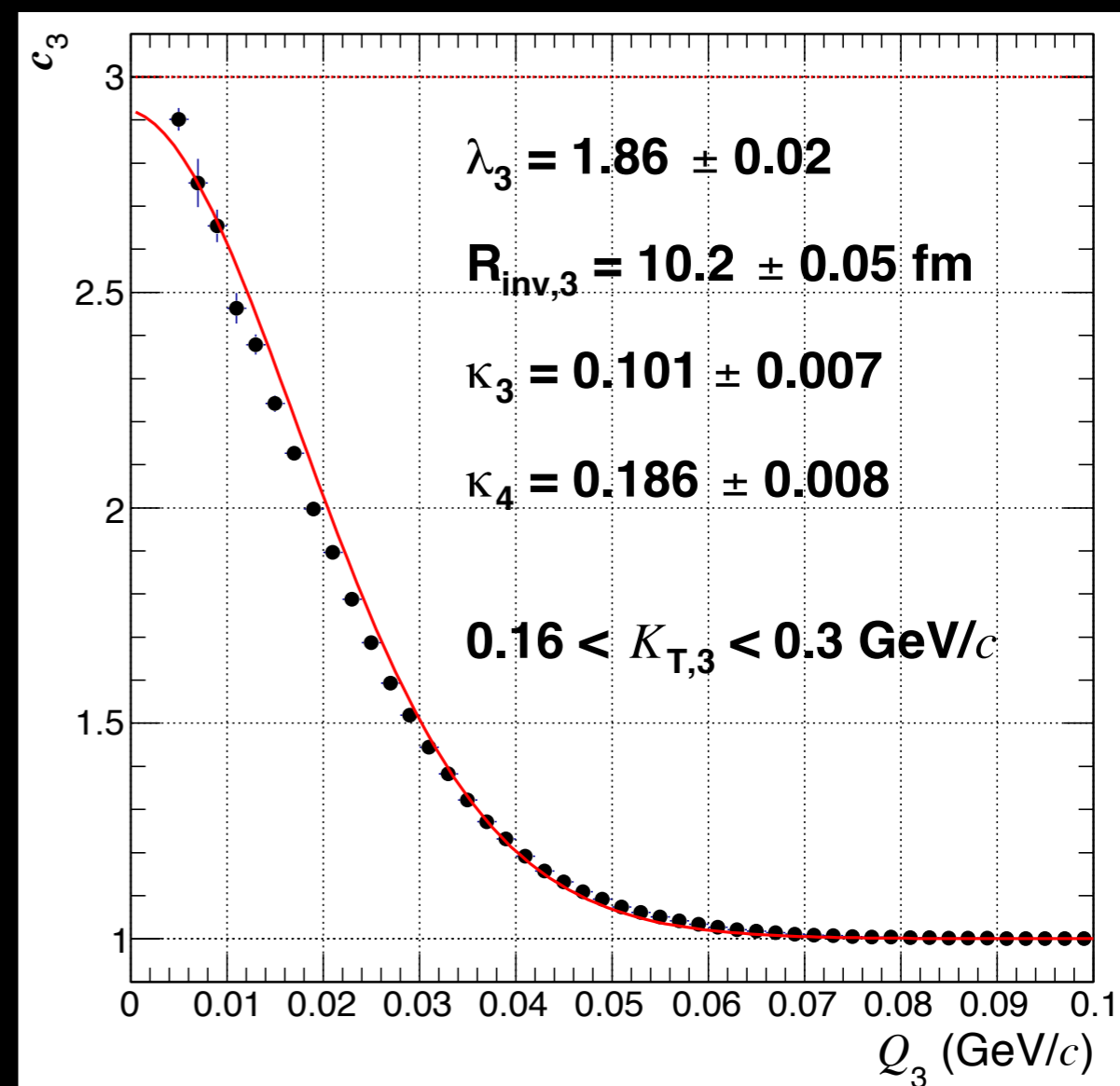
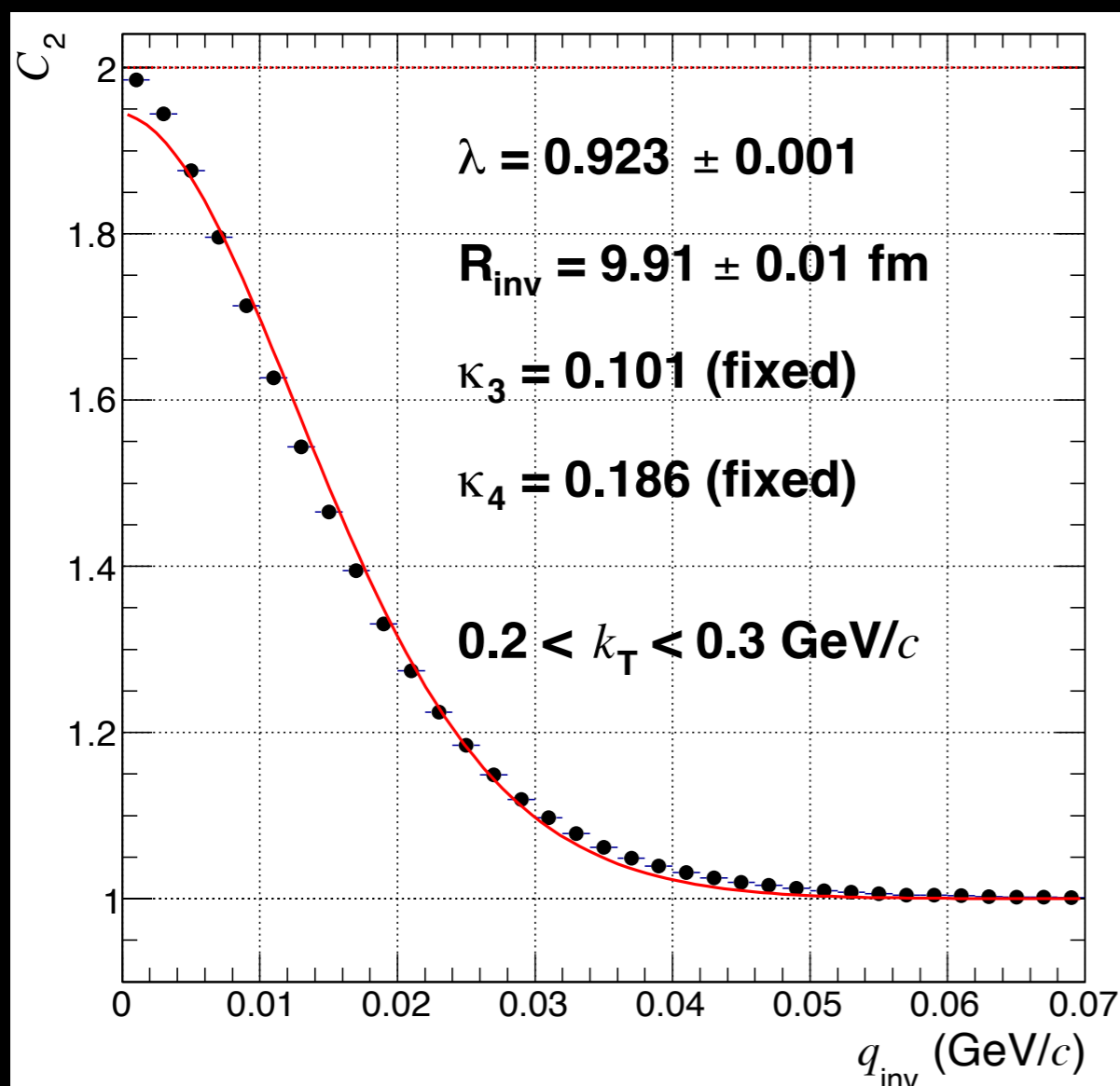


Gaussian fits in **red**.

$R_{inv,3}$ smaller than R_{inv} by $\sim 0.6 \text{ fm}$ (6%).

Therminator 2 model:
Kisiel et al.,
Comput. Phys. Commun. 174, 669
(2006)

Therminator2 calculations of 2- and 3-pion Bose-Einstein correlations



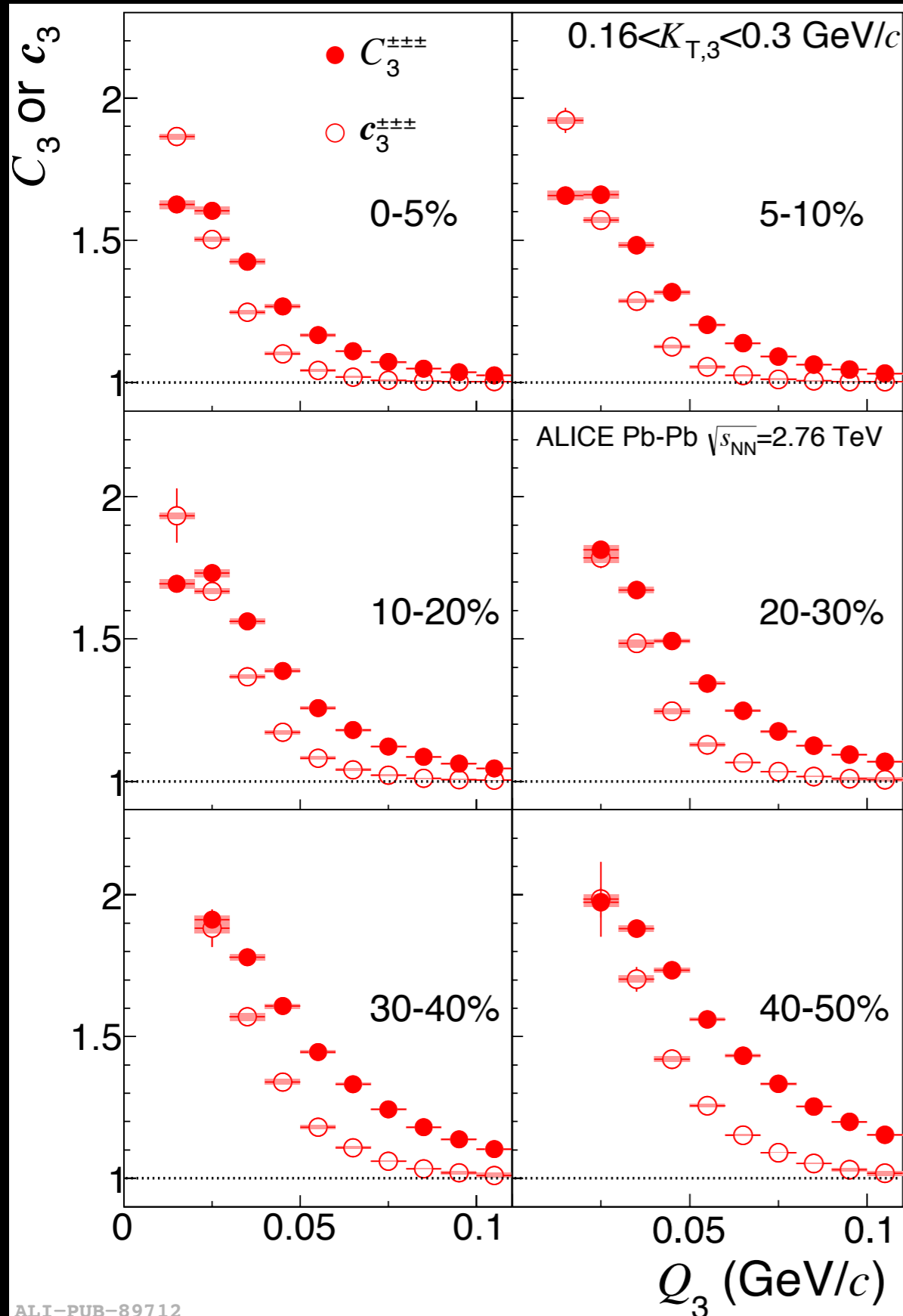
Edgeworth fits in **red**.

$R_{inv,3}$ similar to R_{inv} within $\sim 0.3 \text{ fm}$ (3%).

Therminator 2 model:
Kisiel et al.,

Comput. Phys. Commun. 174, 669
(2006)

3-pion Correlation Functions in Pb-Pb

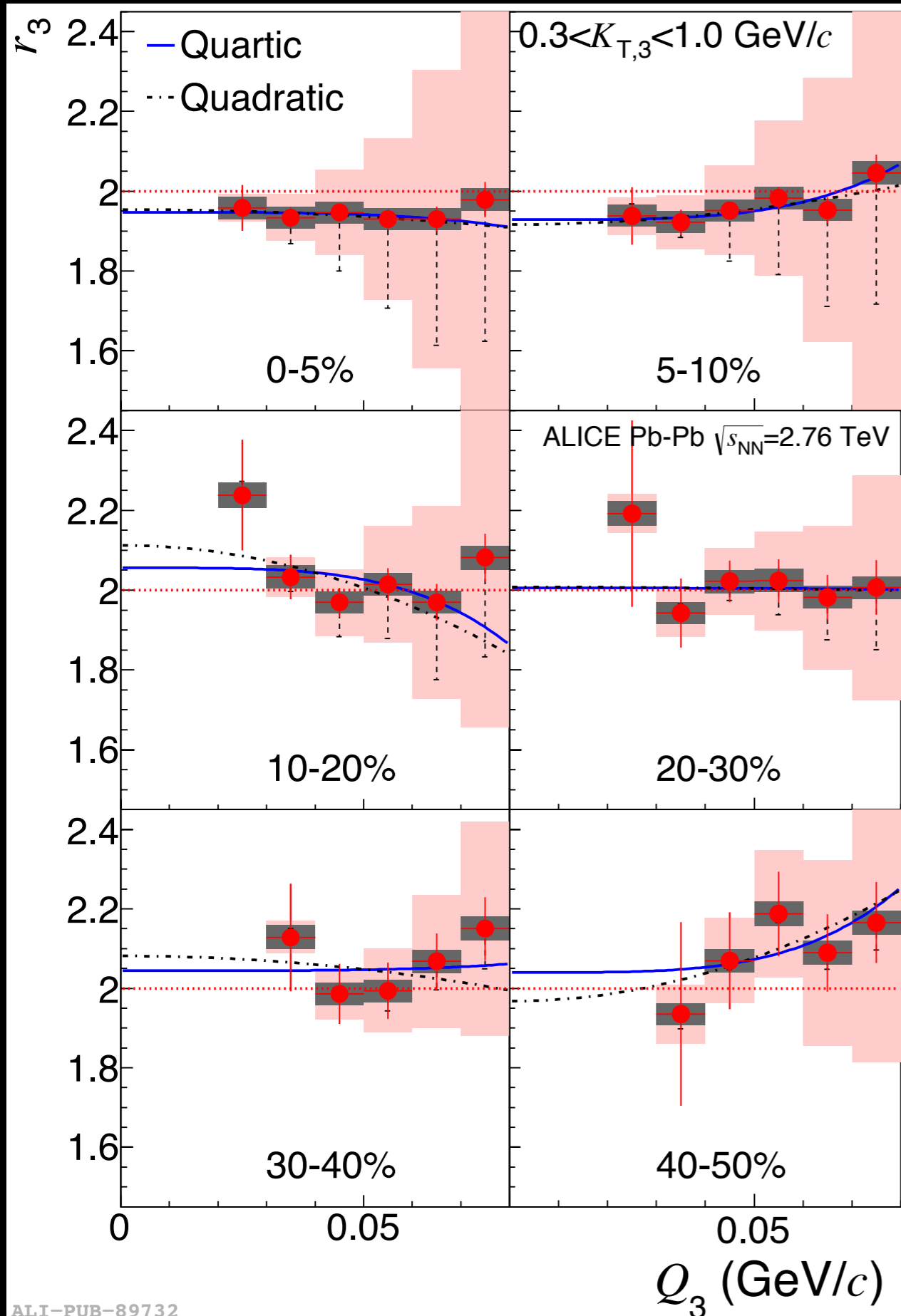


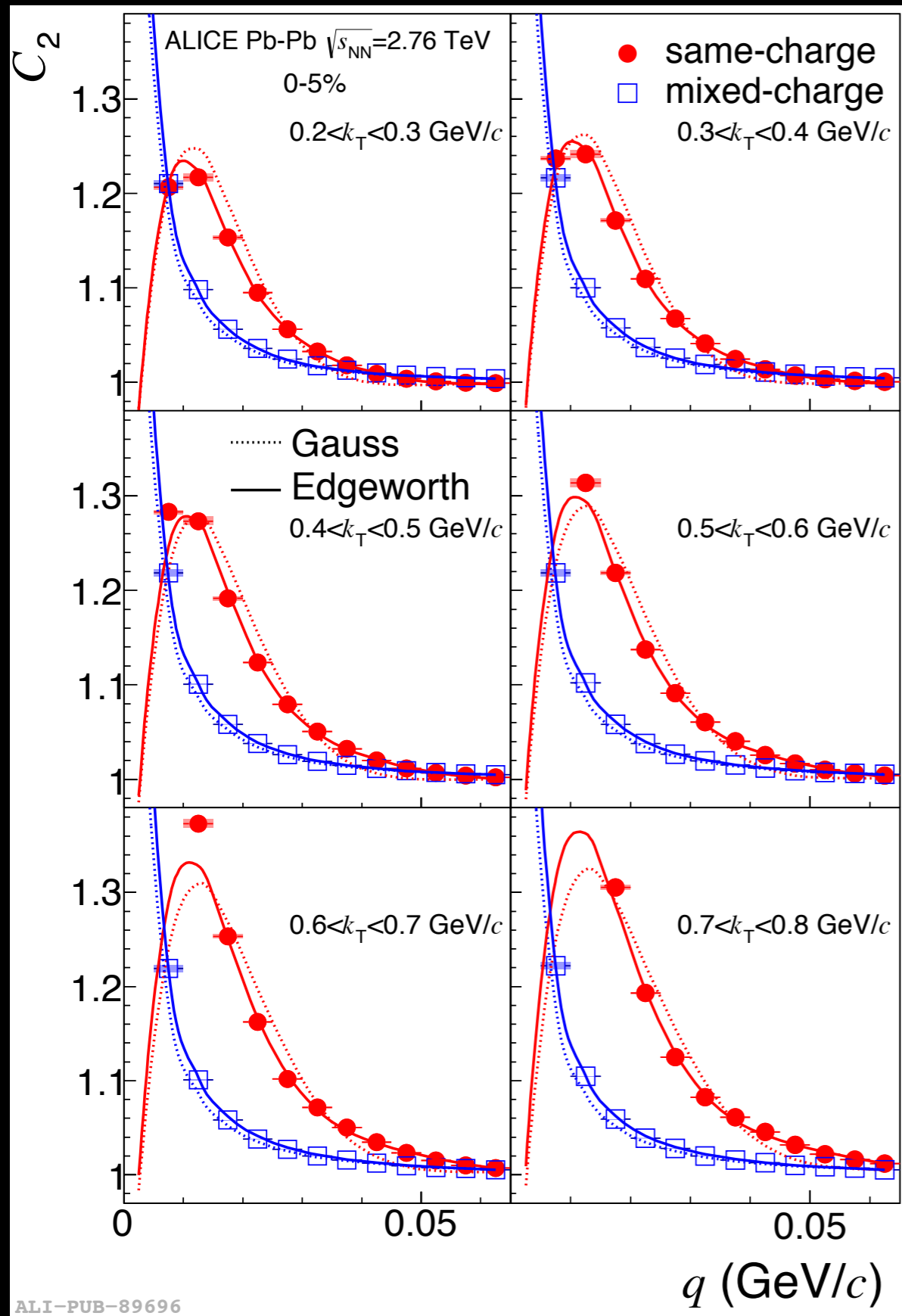
Measure of coherent fraction by comparing 3-pion to 2-pion correlation strength

$$r_3 = \frac{c_3(q_{12}, q_{23}, q_{31}) - 1}{\sqrt{(C_2(q_{12}) - 1)(C_2(q_{13}) - 1)(C_2(q_{23}) - 1)}}$$

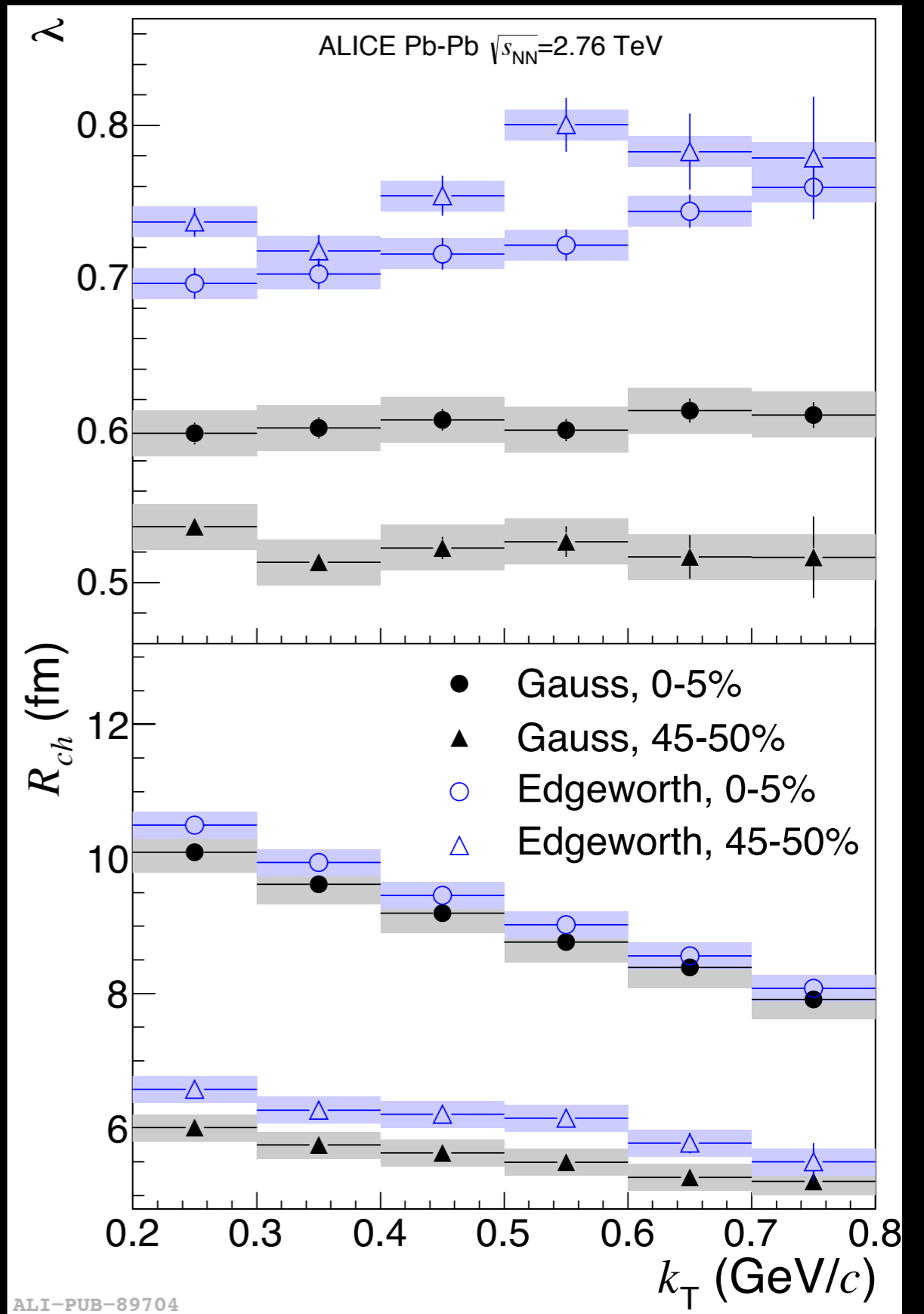
All Correlations are first Coulomb corrected.

r_3 is consistent with 2.0.
Intercept is consistent with **0% coherence at high p_T**





ALI-PUB-89696



ALI-PUB-89704

ALICE
PRC 89 024911 (2014)

Quadruplet Fractions in Therminator

